Journal of Marine Science and Technology
https://doi.org/10.1007/s00773-026-01141-y

REVIEW ARTICLE

Forecasting maritime vessel trajectories: a comprehensive review of data-driven approaches

Lucija Žužić[1,2] · Nikola Lopac[2,3] · Marko Šimic[4] · Jonatan Lerga[1,2]

Received: 10 July 2025 / Accepted: 25 July 2026
© The Author(s), under exclusive licence to The Japan Society of Naval Architects and Ocean Engineers (JASNAOE) 2026

Abstract
Maritime navigation safety is the basis for global logistics and marine ecosystems. The increasing availability of Automatic Identification System (AIS) data has opened new avenues for forecasting vessel trajectories with higher precision and robustness. This review presents a comprehensive survey of recent data-driven approaches, including probabilistic models, classical statistical methods, and deep learning (DL) architectures. Long Short-Term Memory (LSTM), Gated Recurrent Unit (GRU), Recurrent Neural Network (RNN), Transformer-based models, and hybrid systems are evaluated for maritime trajectory prediction. By categorizing studies based on their input features (speed, course, and position) and computational methods, this review highlights methodological trends and performance benchmarks. Additionally, an overview of dataset accessibility and contextual variable use, including weather and wave state, is presented to support future reproducibility. We conclude by identifying gaps and future directions toward explainable and adaptive maritime forecasting systems.

Keywords Trajectory prediction · Vessel forecasting · Deep learning · Maritime safety

1 Introduction

Global maritime safety depends on robust, adaptive systems that process large-scale Automatic Identification System (AIS) data to forecast vessel behavior and ensure regulatory compliance. Over the past decade, technological advances in deep learning (DL), probabilistic inference, and spatiotemporal modeling have enabled the development of a new generation of maritime traffic forecasting systems. As the complexity of marine environments increases due to growing traffic density and environmental variability, conventional rule-based systems are becoming inadequate. This paper surveys the state-of-the-art applications of artificial intelligence (AI) to vessel trajectory forecasting, examining a wide range of models and features.

In this work, we explore which input features are most used and useful, evaluating speed, course, and position represented as latitude and longitude. The dataset evaluation reveals their variation in size, scope, and accessibility. The method overview shows which dominates, with examples of Bayesian, Recurrent Neural Network (RNN), Convolutional Neural Network (CNN), and Transformer models. We conclude by examining how methodological advancements address performance trade-offs, particularly in long-term forecasting and uncertainty modeling.

The most recent contribution, such as the Kolmogorov–Arnold Network (KAN) [1], implemented by Liu et al. [2] for the maritime domain, and the efficient feature representation pioneered by Zhou et al. [3], highlight the importance of explainability and knowledge distillation.

✉ Jonatan Lerga
jonatan.lerga@riteh.uniri.hr

Lucija Žužić
lucija.zuzic@uniri.hr

Nikola Lopac
nikola.lopac@pfri.uniri.hr

Marko Šimic
marko.simic@fs.uni-lj.si

1 Department of Computer Engineering, Faculty of Engineering, University of Rijeka, Vukovarska 58, 51000 Rijeka, Croatia

2 Center for Artificial Intelligence and Cybersecurity, University of Rijeka, Radmile Matejcic 2, 51000 Rijeka, Croatia

3 Department of Electrical Engineering, Automation and Computing, Faculty of Maritime Studies, University of Rijeka, Studentska ulica 2, 51000 Rijeka, Croatia

4 Department for Manufacturing Technologies and Systems, Faculty of Mechanical Engineering, University of Ljubljana, Askerceva 6, 1000 Ljubljana, Slovenia

Published online: 19 August 2026

This survey reveals a clear methodological evolution in maritime vessel trajectory forecasting from handcrafted statistical rules and clustering heuristics toward advanced, data-driven learning systems. Early models, such as Ornstein–Uhlenbeck (OU) processes [4] and Gaussian Process (GP) [5], continue to provide critical baselines and support for uncertainty quantification. Density-Based Spatial Clustering of Applications with Noise (DBSCAN) and other clustering methods [6, 7] are crucial for preprocessing and feature extraction.

The adoption of Long Short-Term Memory (LSTM), Gated Recurrent Unit (GRU), attention mechanisms, and models that integrate positional encoding represents a decisive shift toward dynamic, scalable modeling. Transformer models in newer architectures [8, 9] include examples such as the Spatial-Temporal Sequence to Sequence (ST-Seq2Seq) [10] and Trajectory Bidirectional Encoder Representations from Transformers (TrajBERT) [11] model. Transformers demonstrate superior ability to model sequence dependencies and environmental noise. These architectures further improve accuracy by modeling trajectory data as sequences with attention. This indicates a potential direction for future extensions into Transformer-based or hybrid RNN-attention architectures.

Graph-based methods now represent a promising frontier. Reviewed papers include single-graph approaches and the Graph Attention Network (GAT) [12]. Multi-graph fusion architectures, such as the Spatio-temporal Multi-graphs Convolutional Network (STMGCN) [13] and Spatiotemporal Multi-graph Fusion Network (STMGF-Net) [14], were also covered. These systems outperform earlier baselines in multi-vessel forecasting scenarios, enhancing realism and decision-making capabilities.

Overall, the trend is toward hybrid systems that unify the strengths of traditional and modern approaches. Key areas for future research, as the field progresses, include integrating explainability into AI tools and DL models for model transparency in maritime applications, including Graph Neural Network (GNN) [13, 15] and Transformer architectures [8]. Enhancing domain adaptation and transfer learning across geographies and vessel types would be extremely beneficial. Building larger, curated, and publicly accessible open AIS datasets would lessen the burden on future scientists. Developing hybrid architectures that combine statistical rigor with deep representation learning is valuable, as shown by the results in the reviewed literature. Standardizing evaluation metrics and reporting methods to enable fair and reproducible benchmarking would go a long way toward unifying the research field.

The main contributions of this paper are:

- Surveying trajectory prediction trends from statistical to Transformer-based models.
- Highlighting the rise of graph-based methods for realistic multi-vessel forecasting.
- Comparing input features, such as speed, course, and position, across model types.
- Showing that deep learning models dominate recent research.
- Emphasizing hybrid, explainable systems as key for future maritime forecasting.

This paper consolidates the state of the art in maritime forecasting and provides a practical framework for future developments in intelligent, adaptive vessel-trajectory prediction systems. The rest of the paper is structured as follows: Section 1.1 provides a big-picture overview of the screening process. In Sect. 2 on data, Sect. 2.2 addresses recent concerns about data quality and reliability, including spoofing, and cites relevant rates and counts. Section 2.3 describes data sources, locations, dates, and sizes. Section 3 describes the methodology used by trajectory forecasting papers and the limitations of the current state-of-the-art. In Sect. 4, the discussion in Sect. 4.1 expands into a comparison of purposes and applications. Section 4.2 lists software and hardware requirements and demands, including training and inference time. Section 4.3 deals with interpretability and explainability. Section 4.4 includes values for Average Displacement Error (ADE), Final Displacement Error (FDE), and Root Mean Squared Error (RMSE). Section 5 summarizes the implications of the overview and presents the main ideas for future studies.

1.1 Scope and methodology of this survey

A Scopus search returned 13,296 results for papers with the term trajectory forecasting, and the Institute of Electrical and Electronics Engineers (IEEE) Xplore query returned 1151. After removing duplicates and papers without a Digital Object Identifier (DOI), 11,459 results remained. These papers were manually filtered to exclude those whose text was not in English or was unavailable. Additionally, only papers focused on marine environments and utilizing any of the variables, datasets, and methods detailed in the remainder of this review were considered. This resulted in 24 conference papers and 43 journal articles, published between 2019 and 2025, selected for final review. By summarizing 67 studies from 2019 to 2025 (excluding those by the authors to ensure an unbiased review) categorized by method, input, and feature use, this paper provides a robust roadmap for developing the next generation of maritime forecasting tools.

Figure 1 includes the timeline of papers by year, with the author names and citation number in this paper, from 2019 to 2025.

With 3 papers published in 2019, 7 in 2020, 8 in 2021, and 10 in 2022, the number of reviewed manuscripts has

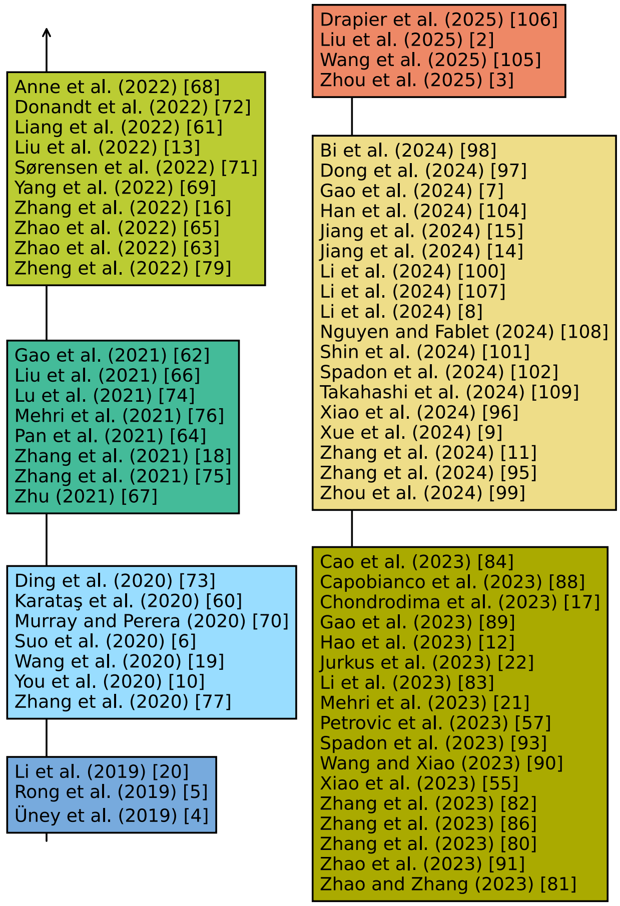

Fig. 1 A timeline of papers by year (2019–2025) with the abbreviated author names, year in brackets, and citation number in this paper in square brackets

shown a steady upward trend. Figure 1 also indicates a rapid increase in research on maritime trajectory forecasting between 2023 and 2025. The upward trend aligns with the increased availability of AIS data and improvements in AI modeling. Peaks in 2023–2025 coincided with the introduction of Transformer-based models. There was a record number of publications from 2023 and 2024, with 17 and 18 summarized papers, respectively. 4 publications were added from 2025, increasing the timeliness and relevance of this review.

2 Dataset

The reviewed studies mostly utilize AIS data as the primary source. The datasets are generally drawn from open seas or specific geographic locations. Some papers use satellite systems other than AIS [16], including Global Positioning System (GPS) [17], whereas others use High-Frequency (HF) radar data [18]. Longitude, latitude, speed, and course are usually studied directly, but some studies have examined images or videos transmitted by satellite to track vessels [19].

However, dataset accessibility varies as most works do not specify direct public access methods since datasets are often proprietary or anonymized for privacy reasons. The authors usually imply proprietary or research-specific acquisition from the North Atlantic Treaty Organization (NATO) Science and Technology Organization (STO) [4], national research institutes, and port authorities. Reproducibility may require contacting the authors or relevant institutions.

Here, we list examples from the reviewed papers to illustrate the various location-specific models. Üney et al. [4] utilized AIS data from the Ionian Sea between April and June 2016. Data were segmented using a 15-by-15 spatial grid to classify trajectories into 128 unique classes. Li et al. [20] employed AIS data from the South Channel crossing waters (Yangtze River Estuary) for July 2017, emphasizing trajectory clustering and prediction. Rong et al. [5] used three months of AIS data representing the Southbound traffic from the Traffic Separation Scheme off Cape Roca in Portugal for uncertainty modeling. Mehri et al. [21] examined vessels around the English Channel using 3,196,110 AIS messages transmitted by 1133 ships during February 2016. The tests by Jurkus et al. [22] are performed on a real historical dataset, exclusively on cargo vessel type trajectories in the Netherlands, around the North Sea coastal region. Jurkus et al. [22] also used data from the Baltic Sea region for validation.

2.1 Automatic identification system

With the adoption of AIS, a significant amount of data on vessel movements has become publicly available. The International Maritime Organization (IMO) enforces various laws to monitor and manage vessel operations and limit harm caused by natural or artificial elements by receiving signals from vessels. These regulations also cover AIS use. AIS is a digital system that provides accurate, real-time static and dynamic information for vessel navigation while tracking the locations of moving marine vessels. Static and voyage-related information is provided every six minutes. However, AIS location reports are broadcast relatively every two to ten seconds, depending on the vessel's speed, and every three minutes if at anchor. As an interface for monitoring maritime traffic, AIS has been used to reduce the likelihood of accidents. Supervisors can get rich insights using AIS combined with radar [18] or other sensors and imaging [19]. The International Convention for the Safety of Life at Sea (SOLAS) has mandated that most commercial vessels, including cargo, passenger, tanker ships, and all those above 300 gross tons, must use AIS [23].

AIS transmissions include columns containing the Maritime Mobile Service Identity (MMSI) number, GPS coordinates (latitude and longitude), Course Over Ground (COG),

Table 1 Part of the header of an AIS message

Column	Description
MMSI number	Vessel identification
Latitude	GPS coordinates, east–west position
Longitude	GPS coordinates, north–south position
COG	The direction of progress between two points
Heading	The direction of a vessel's bow
SOG	The current speed in knots
Status	4-bit number representing navigation status
Timestamp	The time and hour of the day

heading, Speed Over Ground (SOG), status, timestamp, and other vessel- and path-related metadata. The trajectory usually includes a series of AIS transmissions. The heading is the direction in which a vessel's bow points. It is the angle between the north and the vessel's bow. The course represents the vessel's progress between two points. The heading may differ due to wind, tides, and currents. The remainder of the text will use the term course to refer to data sources other than AIS. Part of the header of an AIS message is described in Table 1.

Although AIS has great promise, it is not yet fully utilized. Since they can represent ship motion for forecasting trajectories, position (longitude and latitude), speed, and course are the most frequently used variables. Other information can enhance pattern recognition or enable the filtering of superfluous data and errors, as demonstrated by various preprocessing, clustering, or graph-based techniques in the cited papers.

2.2 Dataset reliability

Detecting unusual vessel trajectories is a topic of significant interest in recent papers. Another relevant topic is unusual AIS behavior, with numerous sources reporting spoofing, jamming, or the presence of dark ships [24]. This demonstrates that unusual vessel trajectories can be reliable and versatile indicators of potentially harmful or dangerous behaviors. This analysis also highlights the susceptibility of AIS data to manipulation by the crew, which has gathered significant concern in recent years. Changing the transmitted latitude, longitude, or MMSI number, or turning off the AIS message transmitter, are examples of anomalous AIS messages on maritime vessels.

Spoofing is the practice of transmitting data that is partially false. It may be used for a variety of attacks, and it has been covered in papers by several authors [25, 26]. The act of transmitting false AIS signals that appear to originate from another vessel is known as AIS spoofing. Spoofing can cause the receiver to detect the vessel's position at a different location. Most anomalous behavior is detected through AIS data. This is why seafarers engaged in illegal activities hide and spoof AIS signals.

However, jamming involves transmitting strong radio signals that obstruct or interfere with the AIS signal. AIS jamming can result in the loss of the received signal, which is comparable to shutting off the AIS transponder. Numerous techniques for detecting these unusual AIS-related activities have been developed in response to the rise in AIS signal spoofing and jamming.

To identify AIS signal spoofing behaviors of vessels, several approaches were used, including Region-based Convolutional Neural Networks and k-Nearest Neighbors (k-NN) [27], OU process [28], CNN [29], and GP methods [30]. Zhang et al. [31] also suggested using vessel trajectories to identify signal-spoofing behaviors. The position and time transmitted by the vessel are crucial characteristics for identifying AIS signal spoofing activities. AIS data were often used to determine a vessel's position from its latitude and longitude.

Some research from 2018 and 2019 [27–29] classified vessels as dark ships if they turned off their AIS facility during the journey. Because AIS equipment is manipulable and can be turned on and off to conceal illicit activity, the AIS On-Off Switching (OOS) anomaly is crucial to maritime security. There are two main methods for spotting dark ships. In the first, AIS data is contrasted with information obtained from other sources, including satellite images [27], radar [28], and Synthetic Aperture Radar (SAR) [29]. However, only AIS data is taken into account by Shahir et al. [32], Singh and Heymann [33], and Mazzarella et al. in 2016 and 2017 [34, 35]. The detection of dark ships is challenging because intentional AIS transponder shutdowns and equipment malfunctions can cause signal loss. By accounting for the vessel's long-term trajectory and comparing it with the intended track, this problem can be mitigated to some extent [28].

Singh and Heymann [36] conducted a comparative analysis of AI approaches to assess their effectiveness in identifying AIS OOS anomalies in the marine domain. Artificial Neural Network (ANN), Support Vector Machine (SVM), logistic regression, k-NN, decision trees, Random Forest (RF), and naive Bayes are the seven AI approaches used in the cited papers to detect and differentiate between intentional and non-intentional AIS OOS abnormalities. According to experimental results, ANN and SVM are the most effective methods, with a 99.9% accurate detection of AIS OOS anomalies. When training on a balanced dataset with equal numbers of samples per class, the ANN model performs better than the others. In contrast, SVM is the top performer on an unbalanced training dataset.

Using OU mean-reverting processes (piecewise), d'Afflisio et al. wrote studies in 2021 [37, 38] to propose an efficient anomaly detection procedure that reveals AIS data spoofing and/or covert stealth deviations from the planned nominal route by reporting adulterated position information about the vessel's current route. The framework is supported by trustworthy data from monitoring systems, more precisely, coastal radars and spaceborne satellite sensors.

Shahir et al. detect AIS spoofing activities by first identifying the endpoint of the vessel trajectories using DBSCAN [32]. Shahir et al. do not use data sources besides AIS, such as radar [28], SAR [29], or satellite images [27], when searching for dark ships. After obtaining the data, the authors compare a vessel's trajectory to historical patterns. Vessel type was employed by Ford et al. [39] and Shahir et al. [32] in their learning algorithms. These works have shown that vessel type can be inferred from other AIS characteristics, including flag state and status.

Prasad et al. [26] introduced a novel shipping-route extraction technique for processing historical AIS data, characterizing global shipping route behavior, and capturing seasonal trends. Other use cases are also discussed, such as identifying different anomalies in the behavior of a single vessel, including spoofing, intentional or unintentional AIS OOS, and departures from the shipping lane. Using DBSCAN clustering and a region-based algorithm, spoofing points across several categories are identified.

According to the International Electrotechnical Commission (IEC) and IMO Resolution 61108 A.1046(27), detailing the Satellite-Based Augmentation System (SBAS) standard for shipborne receivers [40], a positioning accuracy of approximately 10 m is required for maritime navigation [41], so it is necessary to improve data quality for real-time applications. Inland waterways are narrow, requiring errors to be reduced to 5 m, so these applications often use Differential Global Navigation Satellite System (DGNSS) corrections [41].

R-Mode has been proposed as a backup to the Global Navigation Satellite System (GNSS) [42], thereby providing technical solutions to mitigate spoofing and interference and providing a baseline for assessing the sensitivity of systems to these errors. After trajectories have been divided into segments, the isolation forest algorithm has been shown to successfully identify spoofed ships, with accuracies ranging from 76.4% (24.6% missing-point ratio) to 100% (4.1% missing-point ratio) [43].

As spoofing can affect an aircraft in addition to a watercraft, a study was conducted in the area near Graz Airport in the 5 months from 08.10.2024 to 07.01.2025 [44]. The mean number of events ranged from 1.43 to 9.08, depending on the month and the quarter of the day, and the mean duration was between 7.41 s and 63.24 s [44]. The minimum number and duration of events occurred between 00:00 and 06:00, and the interferer may have moved more quickly due to sparse traffic, which may explain this deviation [44].

The GPSPATRON website reviewed various open sources to produce a report [45], which documented events categorized by 5 high-risk areas, as shown in Table 2. They found that more events occurred in 2025 than in any of the 4 preceding years, largely due to geopolitical events and instability in Eastern Europe and Asia [45].

Elaborating on the previously reported counts by region and focusing on the maritime domain, the GPSPATRON report [45] also lists the number of events for vessels in the last three quarters of 2024 and the first two quarters of 2025. The estimated number of vessels affected by maritime GNSS interference was 227, 550, 120, 1405, and 10,660 for 2024 Q2, 2024 Q3, 2024 Q4, 2025 Q1, and 2025 Q2, respectively [45]. The number of events was more than 10 times larger in 2025 than in 2024 despite a longer time range in 2024, suggesting that the total number could be much higher [45].

These combined reports lead us to conclude that threats are imminent and on the rise, with an increasing number of dangerous events [44, 45]. However, there are viable solutions to identify polluted data [43] and remove it from the training set for a trajectory prediction model. There are also viable alternatives to GNSS [42] for ships navigating in risky conditions, ensuring that passengers and cargo are not jeopardized.

2.3 Dataset accessibility

The general public can get a visualization of real-time AIS data for free from the MarineTraffic [46] website. The AIS Dispatcher [47] is an AIS data-forwarding utility that provides free access to real-time AIS raw data but does not provide access to historical records. Different sources for downloading AIS historical data can be found in a paper by Kress and Mitchell [48], such as the United States Coast Guard (USCG) AIS Historical Requests [49], Marine Cadastre [50], SeaVision [51], Maritime Safety and Security Information System (MSSIS) [52], Global Maritime Traffic Density Service [53], Environmental Systems Research Institute (ESRI) Living Atlas, and United States (US) Vessel Traffic [54]. Individual vessel data or coverage of geographic areas can be downloaded from these sites. Some sources cover global traffic, but the spatial coverage is often limited. Instead of an immediate download, a waiting time is sometimes unavoidable and varies with the size of the desired dataset. Certain sources impose various use and access restrictions, often requiring registration.

Data from Marine Cadastre [50] contains vessel movement data collected by the USCG and is a widely used [17,

Table 2 The number of reported and documented maritime GNSS interference incidents by region and year (2021–2025), extracted from reports and recorded events [45]

Year	Black Sea	Baltic Sea	Eastern Mediterranean	Red Sea	Persian Gulf/Hormuz
2021	1	0	0	0	1
2022	4	1	0	0	1
2023	4	3	1	0	1
2024	10	8	4	2	0
2025	12	10	1	2	6

55], freely accessible, and publicly available source for open AIS data from US waters.

We found examples that analyzed trajectories near Brest and in the Aegean Sea, [17] extracted from the vast array of possibilities. The Brest dataset [56] includes over 18 million AIS records collected in French waters.

The dataset used by Petrovic et al. [57] contains valuable metadata and is publicly available from Kaggle [58]. The data describe traffic in the Kattegat Strait and contain 10 columns from the AIS headers, including vessel MMSI numbers, navigational status, SOG, COG, vessel heading, width, length, and draft.

The Association for Computing Machinery (ACM) International Conference on Distributed and Event-Based Systems (DEBS) 2018 Grand Challenge dataset [59] is still a relevant resource, used by Karataş et al. in 2020 [60]. This dataset contains AIS messages between 10 March and 19 May 2015. The ACM DEBS 2018 Grand Challenge was the eighth installment of a challenge series that provides a common platform and evaluation system for contests that solve academic and industrial problems. The goal of the 2018 Grand Challenge was to use machine learning (ML) with space-time data streams as input to increase safety in marine transportation by forecasting vessels' destinations and arrival times. The approximate dataset size is 503 distinct ships and 540,000 rows. The data contain AIS messages from the Mediterranean, but those from European coasts are overrepresented. The dataset comprises 20 vessel types, predominantly cargo ships.

Before presenting the results for each state-of-the-art paper, we examine the data characteristics, including locations. The South Channel [20, 61] and the Jiangsu section [62] are frequently studied in the Yangtze River Estuary [63] owing to their dense traffic, which provides rich AIS data and coverage. Zhangzhou Port [6], Huanghai [18], L Port [64], and Yangshan Port [63, 65] were also among the many Chinese locations included in the covered related work. Also in China, You et al. [10] studied the Wuhan and Chongqing Waterway, while Wang et al. [19] focus on the sea near Hong Kong. Liu et al. [66] cover three areas in China: the Caofeidian Coastal Waters (CCW), the Chengshan Jiao Promontory (CJP), and the Zhoushan Islands (ZSI). Another Chinese study [13] examines the Tianjin Port (TJP), Luotou Waterway (LTW), and Qiongzhou Strait (QZS). Zhu [67] focuses on the area near Laotieshan, also in China.

In other parts of the Eastern hemisphere, the Indonesian Maritime Security Agency (originally Badan Keamanan Laut (Bakamla)) provides data on the Indonesian Archipelagic Sea Lanes (originally Alur Laut Kepulauan Indonesia I (ALKI 1)), covering an area from Singapore to Tanjung Priok (Jakarta), as evident in the work by Anne et al. [68]. Yang et al. [69] also focus on East Asia, specifically Taiwan.

In European studies, notable locations include the Ionian Sea [4] and Cape Roca in Portugal [5]. Karataş et al. [60] make use of the DEBS 2018 [59] data and cover the Mediterranean Sea and European Coast. Murray and Perera [70] move toward Scandinavia, relying on the Norwegian Coastal Administration and source data from Tromsø, Norway. Sørensen et al. [71] use data collected in waters to the west of Norway. Donandt et al. [72] focus on inland waterways, covering the Danube river, according to data provided by the German Federal Waterway Engineering and Research Institute (originally Bundesanstalt für Wasserbau (BAW)).

Also on the Western hemisphere, Marine Cadastre [50] is a reliable source of information for studies of American waters [73, 74], along with the USCG [49, 75]. Mehri et al. [76] used the National Oceanic and Atmospheric Administration (NOAA) [76] as the source of information on the Eastern United States (US) Coast. The type, source, location, time span, and size for each dataset referenced from 2019 to 2022 are listed in Table 3 for a more detailed overview of these summarized findings. Zhang et al. [16] use satellite data and focus on a cargo ship, as the data is provided by MAERSK, one of the largest worldwide shipping companies. Wang et al. [19] also use satellites, while Zhang et al. [18] rely on radar.

There are valuable examples [18, 19] proving that the options are not limited to AIS alone. As there is a great diversity in the dataset size as well as the locations, with Zhang et al. [77] covering only 90 AIS trajectories, while Liang et al. [61] use as many as 49,532 trajectories, a direct comparison of these results would be unfair due to the vastly different scales, which must be considered when evaluating cross-study metrics. Hao et al. [12] and Zhang et al. [80] focus on Shanghai. Zhao and Zhang [81] use 5 self-developed datasets in Zhoushan and Ningbo (China), whereas Zhang et

Table 3 Papers (2019–2022) with data types, sources, the place and time of gathering, and size

Description
Li et al. [20]: South Channel, Yangtze, July 2017, 237 trajectories
Rong et al. [5]: Cape Roca, Portugal, 01.10.–31.12.2015, 1396 trajectories
Üney et al. [4]: Ionian Sea, 01.04.–01.06.2016
Ding et al. [73]: Marine Cadastre [50], 32° N to 42° N and 126° W to 120° W, Time: 2017, 36,000 segments
Karataş et al. [60]: DEBS 2018 [59], Mediterranean Sea and the European Coast, 10.03.–19.05.2015, 540,000 rows
Murray and Perera [70]: Norwegian Coastal Administration, Tromsø, 01.01.2017-01.01.2018, 15 million points
Suo et al. [6]: Zhangzhou, China, 7,577,484 points
Wang et al. [19]: Google Earth and the Jilin-1 Satellite, Hong Kong, 8022 images and 1300 frames
You et al. [10]: Wuhan (30.22° N to 30.7° N and 114.05° E to 114.5° E) and Chongqing (29° N to 29.62° N and 106° E to 106.61° E) Waterway, 01.–10.06.2017
Zhang et al. [77]: 90 trajectories
Gao et al. [62]: Jiangsu, Yangtze, 1000 trajectories
Liu et al. [66]: Caofeidian Coastal Waters (CCW), Chengshan Jiao Promontory (CJP), and Zhoushan Island (ZSI)
Lu et al. [74]: Marine Cadastre [50], America (ocean)
Mehri et al. [76]: NOAA [78], Eastern US Coast, Nov. to Dec. 2017, 58,545,206 records (10,676 vessels)
Pan et al. [64]: L Port, China, 1 month, 277 trips
Zhang et al. [18]: AIS and radar, Huanghai, China, Yellow Sea, 20.07.2019, 3 AIS traces (1652, 1802, and 1002 points)
Zhang et al. [75]: USCG [49], Area 18, January 2016, 136,430 sampling points
Zhu [67]: Laotieshan
Anne et al. [68]: Bakamla, ALKI 1 from Singapore to Tanjung Priok, July to Sep. 2022, 154,893 rows
Donandt et al. [72]: BAW, Danube river (2231.4 to 2321.44 hectometers), May 2019 to Sep. 2021, 7.7k trajectories (250k-280k sequences)
Liang et al. [61]: South Channel, Yangtze (31°07′ N to 31°34′ N and 121°23′ E to 121°59′ E), 31.07.–31.08.2017, 49,532 trajectories/61,994,075 points
Liu et al. [13]: Tianjin Port (TJP), 1942 trajectories/7,503,278 points, Luotou Waterway (LTW), 3603 trajectories/12,912,115 points, and Qiongzhou Strait (QZS), 4069 trajectories/7,572,283 points, 01.–30.07.2018
Sørensen et al. [71]: Gatehouse Maritime/exactEarth satellites, west of Norway (320,000 square km), June to Aug. 2016–2019, 113,788,768 messages (3631 cargo ships)
Yang et al. [69]: Taiwan (20° N to 25° N and 120° E to 123° E), 06.07.2019 + 1-month navigation track data, 1,048,575 points/1364 vessels
Zhang et al. [16]: Satellite, MAERSK, 2011–2015, 18,458 (trajectory data)
Zhao et al. [65]: Public data and merchant websites, Yangshan (Xiaomei/Shenjiawan Passenger Terminal), 01.11.–06.11.2019, 3 ship trajectories
Zhao et al. [63]: Merchant websites, Yangshan Port and the Yangtze River Estuary (inside and outside), 18.12.2020, 04:30–10:00 (Yangshan), 07:00–13:00 (Yangtze), and 09:00–13:00 (outside)
Zheng et al. [79]: East US Coast, 6000 track points

al. [82] combine datasets from the US and China. Li et al. [83] once again cover the Chengshan Jiao Promontory, Zhoushan Archipelago, and Caofeidian Port, just as they did in their prior study in 2021 [66]. Cao et al. [84] present a study on a global dataset spanning the largest longitude and latitude ranges, once again highlighting the importance of diversity. Chondrodima et al. [17] use a highly diverse dataset, sourced from MarineTraffic (Aegean Sea) [46], Marine Cadastre (US West Coast) [50], and the French Naval Academy (Brest).

The time span also has a huge impact on results, as Xiao et al. [55] provide an interesting perspective on the effect of the Coronavirus Disease 2019 (COVID-2019) on worldwide shipping, using data both before and after the most intensive crisis periods from Marine Cadastre [50] on the US West Coast, and supplement with data from the Danish Maritime Authority (DMA) [85] on Denmark's Strait. Petrovic et al. [57] also use data from Marine Cadastre [50] on a single vessel, but supplement it with the DEBS 2018 challenge. Zhang et al. [86] use the Marine Cadastre [50] data on the South Western and South Eastern US Coast. Mehri et al. [21] study the English Channel. Jurkus et al. [22] use ShipFinder [87] in the Netherlands (North Sea), as well as the DMA [85] on the Baltic Sea near the island of Bornholm. Capobianco et al. [88] also use the DMA data [85] to study the Danish Universal Transverse Mercator (UTM) zone 32V. Gao et al. [89] combine data from Copenhagen and Yangshan, demonstrating that European and Asian sites can be combined to improve coverage.

Wang and Xiao [90] use public Yangtze River Estuary data, and Zhao et al. [91] use ChinaPorts (no longer available outside mainland China) for a Yellow Sea and Yangtze study. This status change demonstrates that fragile political circumstances can create a dichotomy and abruptly disconnect researchers from global data, forcing them to seek alternatives, such as HiFleet [92]. Some resort to private intelligence, as Spadon et al. [93] use Spire [94] data for the Atlantic Ocean.

Data from 2023 in Table 4 and from 2024–2025 in Table 5 once again include many studies on the Yangtze River [95, 96] and Jiangsu [7], as well as Zhoushan Island [66, 81, 83] and Yangshan [12, 14, 89], as also covered in studies from 2022 [63, 65]. Additional Chinese studies cover the Wenzhou Fishing Vessel Safety and Rescue Center [9] and ShenZhong [97]. Bi et al. [98] and Jiang et al. [15] also focus on Asian data. Zhang et al. [11] are broader in scope, covering Europe, the Middle East, Asia, and Africa.

Marine Cadastre [50] is once again the prime domain for US data in 2024 [99–101] on the Pacific and Atlantic Coast. Spadon et al. [102] also focus on North America and study the Gulf of St. Lawrence in Canada, but they use data from Spire [94], a commercial source.

As demonstrated by Table 5, in Europe, IEEE DataPort [103] contains data on the Baltic Sea, and the Norwegian Coastal Administration (originally Kystverket) [104] is the main authority for its national dataset, as is the DMA [85] for Denmark.

The large diversity observed in the locations, creation times, and sizes of the data in Table 5 once again demonstrates that a direct comparison is not viable. While a 2025 paper uses DMA data [85, 105], another combines it with the USCG information [3, 49]. 0ne paper uses French Navy proprietary data [106], and another is focused on polar ships [2]. However, the analysis also shows that data collection is highly concentrated in a few areas of interest.

The limited options represented in popular public datasets suggest that a broader effort to gather information beyond high-traffic ports could yield novel insights in future. Because AIS, satellite, and radar data are not always sufficient to capture environmental conditions, additional contextual data are needed, as detailed below.

2.4 Contextual data

To improve trajectory forecasting, additional real-world information about the vessel and its environment may be helpful. Various environmental factors [21], including sea and wave state (direction, height, depth, and speed), the distance from the coast, wind conditions (speed, direction, and force), air density, and vessel characteristics (type, hull design, dimensions, weight, and length) are just some of the factors contributing to vessel movement. The temperature, cloud cover, wind speed, and time of day may provide additional insight. Various data sources are used for live or static vessel data [92, 110, 111], natural, environmental, meteorological, and oceanographic data [31, 112], and for data concerning human-related activities [113]. Mehri et al. [21] use vessel type, wave direction, height, length, water depth, wind speed, and direction as contexts. The Meteorological Aerodrome Report (METAR) data, including temperature and wind speed can be obtained from *r5.ru* [114]. Ocean states measured by satellites at different levels of preprocessing can be obtained from the Copernicus Marine Environment Monitoring Service (CMEMS) and the Copernicus Climate Change Service (C3S) [115].

Additional details on contextual and environmental datasets reported in the reviewed literature are provided in Table 6, including dataset types, sources, data collec-

Table 4 Papers (2023) with data types, sources, the place and time of gathering, and size

Description
Cao et al. [84]: Global (40° S to 80° N and 150° W to 150° E), 25.07.2021 15:10–18:59
Capobianco et al. [88]: Source: DMA [85], Denmark UTM zone 32V, Jan. to Feb. 2020, 394 trajectories (8574 (train), 1054 (validation), and 2379 (test) sequences)
Chondrodima et al. [17]: MarineTraffic [46], Marine Cadastre [50], and the French
Naval Academy, Aegean Sea [46] (36.0846° N to 39.4871° N and 24.4556° E to 26.5869° E), 01.–30.11.2018, 1,289,642 records (2854 vessels), US West Coast [50] (30° N to 50° N and 126° W to 120° W), 01.–28.02.2009, 10,671,963 records (1122 vessels), and Brest (45° N to 51° N and 10° W to 0° W), 01.10.2015–31.03.2016, 18,657,858 records (5041 vessels)
Gao et al. [89]: Copenhagen (55.65261° N to 55.75261° N and 12.61431° E to 12.71431° E), 08.02.2022, 19.03.2022, and 13.04.2022, and Shanghai (Yangshan) (30.35364° N to 30.75364° N and 122.18234° E to 122.78234° E), 01–09.07.2022
Hao et al. [12]: Shanghai, China (Yangshan Port) (30.975979° N to 31.631133° N and 122.875756° E to 124.192223° E) and the Taiwan Strait (23.99471° N to 25.920078° N and 118.493770° E to 120.167215° E), 04.07.2022
Jurkus et al. [22]: ShipFinder [87], Netherlands, North Sea coastal region, Sep. 2018 to Feb. 2019, approximately 5,000,000 records, DMA [85], Baltic Sea, Bornholm (54° N to 56° N and 12° E to 15° E), June to Dec. 2021, 11,478,975 records (459,159 generated sequences)
Li et al. [83]: Chengshan Jiao Promontory (37.1667° N to 37.7500° N and 122.5833° E to 123.1667° E), July 2018, 4967 trajectories (3,795,208 points), Zhoushan Archipelago (29.5607° N to 31.0994° N and 121.5056° E to 123.6126° E), 23.–24.04.2018, 7612 trajectories (7,890,322 points), and Caofeidian Port (38.7167° N to 39.1166° N and 118.25° E to 118.9167° E), 01.–10.06.2018, 3606 trajectories (5,936,451 points)
Mehri et al. [21]: English Channel, February 2016, 3,196,110 messages (1133 ships)
Petrovic et al. [57]: Source: DEBS 2018 [58] and Marine Cadastre [50], US and international waters [50], 29,397 (test set) [58] and 1 vessel [50], Date: 31.03.2022 [50]
Spadon et al. [93]: Source: Spire [94], the Atlantic Ocean (23° 52′14.8″ N to 68°30′02.8″ N and 82°46′58.2″ W to 2°01′18.4″ W), Mar. to July 2020, 60,000,000 messages, 20,000+ ships
Wang and Xiao [90]: Source: Public-accessible databases, Yangtze River Estuary, 18.–23.10.2022, 627 points (Ship-1: 276/Ship-2: 351)
Xiao et al. [55]: Marine Cadastre [50], US West Coast (24.5205° N to 49.6551° N and 126.106° W to 117.1515° W), 01.–07.12.2019 (before COVID-19) and 01.–07.12.2020 (after), original AIS data 2,730,919 (before) and 2,579,721 (after), DMA [85], Denmark's Strait
Zhang et al. [82]: US and China
Zhang et al. [86]: Marine Cadastre [50], South Western and South Eastern US Coast (20.91° N to 49.21° N and 125.35° W to 59.56° W), 2021, 144,445,580 points (28,645 vessels)
Zhang et al. [80]: Shanghai Port (30°30.319′ N to 31°37.628′ N and 121°19.224′ E to 122°32.584′ E), 15–18.05.2019, 243,423 data points

Table 4 continued

Description
Zhao et al. [91]: ChinaPorts, Yellow Sea 1 (29.97° N to 37.30° N and 121.73° E to 122.88° E), 19.–21.05.2022, Yangtze (29.93° N to 31.24° N and 121.78° E to 122.32° E), 22.–23.04.2022, and Yellow Sea 2 (22.98° N to 29.46° N and 116.6° E to 122.04° E), 18.–21.04.2022
Zhao and Zhang [81]: Self-made datasets, Zhoushan and Ningbo (China), 23.12.2022.–22.01.2023, 5 datasets

Table 5 Papers (2024–2025) with data types, sources, the place and time of gathering, and size

Description
Bi et al. [98]: 34.4° N to 35.47° N and 119.17° E to 120.41° E, Jan. to Dec. 2022, 2 million records
Dong et al. [97]: ShenZhong Link Management Center, ShenZhong Link (Southern China), 25.–31.04.2024, 1437 data points
Gao et al. [7]: Jiangsu, Yangtze (31.87704° N and 118.54278° E), 13.10.2019
Han et al. [104]: Norwegian Coastal Administration (Norwegian: Kystverket), Horten to Moss, Jan. to Feb. 2019, 236 encounters
Jiang et al. [15]: Source: IEEE DataPort [103], Place: Baltic Sea (53° N to 67° N and 9° E to 31° E), 2017–2019, 1 million AIS records (1851 independent vessel trajectories)
Jiang et al. [14]: Zhoushan Island (29.75° N to 30.1° N and 121.8° E to 122.35° E), 841,943 (AIS data volume), Yangshan Waters (30.35° N to 30.83° N and 121.85° E to 122.65° E), 979,744 (AIS data volume), Yangtze River Waters (31.07° N to 31.6° N and 121.3° E to 122.3° E), 642,594 (AIS data volume), 01.–31.05.2019
Li et al. [100]: Marine Cadastre [50], Place: Pacific Coast (Gulf of California), Atlantic Coast (Chesapeake Bay, Narragansett Bay, and East US Coast), and the Northern Gulf of Mexico, Nov. 2022 to Feb. 2023, 42 vessels (average 874 points per vessel)
Li et al. [107]: ChinaPorts, Fujian Inshore Area (24.6° N to 27.1° N and 119.6° E to 121.7° E), 16.–26.03.2024, 13,679 points
Li et al. [8]: AIS data Nguyen and Fablet [108]: DMA [85], 55.5° N to 58° N and 10.3° E to 13° E, 01.01.–31.03.2019, approximately 712 million AIS messages
Shin et al. [101]: Marine Cadastre [50], US Houston Texas Port (27.8° N to 29.8° N and 95.25° W to 94.25° W), Jan. 2017, 15,920,106 AIS messages (44,611 samples of 1217 vessels)
Spadon et al. [102]: Satellite and AIS from Spire [94] and MERIDIAN, Gulf of St. Lawrence, Canada, 2015–2020, 953 cargo and 391 tanker vessels (train), 51 cargo and 21 tanker vessels (validation), and 252 cargo and 103 tanker vessels (test)
Takahashi et al. [109]: Japan, Pacific (34° N to 40° N and 138° E to 150° E), 01.–07.12.2020
Xiao et al. [96]: Yangtze River, 17.03.2023, 6,057,648 AIS records (1578 trajectories)
Xue et al. [9]: Wenzhou Fishing Vessel Safety and Rescue Center, 26.31° N to 29.88° N and 120.82° E to 126.63° E, 01.–31.01.2016, 12,808 tracks
Zhang et al. [11]: Europe, Middle East, Asia, and Africa, 2016, 23,110 trajectories

Table 5 continued

Description
Zhang et al. [95]: Southern Yangtze River Estuary
Zhou et al. [99]: Marine Cadastre [50], US West Coast, June 2023, 16.3 GB
Drapier et al. [106]: French Navy (proprietary), 84.88° S to 90° N and 180° W to 179.65° E, Aug. 2023 (1 week) and Feb. 2024 (3 days), Size: 1,746,686 trajectories
Liu et al. [2]: GNSS, Xue Long 2 (Arctic) and Tian Hui (Antarctic) navigation records, 28.07.–09.08. 2024 (Arctic route) and 08.11.–14.12.2023 (Antarctic route)
Wang et al. [105]: DMA [85], 55.5° N to 58° N and 10.3° E to 13° E, 02.01.–24.02.2024, 98,304,795 records
Wang et al. [105]: AIS (ship performance), DMA [85], 55.5° N to 58° N and 10.3° E to 13° E, 02.01.–24.02.2024, 3648 records
Zhou et al. [3]: DMA [85], Kattegat (55.5° N to 58° N and 10° E to 13° E), July 2022, 6257 vessels, USCG [49], Gulf of Mexico (21° N to 30° N and 97° W to 84° W), 28.9.2022

tion locations and times, and approximate sizes. The French Oceanographic Office (originally Service Hydrographique et Océanographique de la Marine (SHOM)) and the French Research Institute for Exploitation of the Sea (originally Institut Français de Recherche pour l'Exploitation de la Mer (IFREMER)) provide valuable hydrographic data for Mehri et al. [21]. Zhou et al. [3] use Organic Matter Aerosol Optical Depth at 550 nm (OMAOD550) for additional enrichment of their environmental model. The European Center for Medium-Range Weather Forecasts (ECMWF) fifth-generation dataset (ERA5) is also a part of CMEMS.

World Weather Online is used by Wang et al. [105] in their study of wave, wind, and temperature conditions. As can be seen in Table 6, a relatively small subset of papers use contextual information, which is a flaw that must be corrected, as richer input could yield novel insights and better capture environmental nuances affecting navigation.

2.5 Feature selection

All reviewed studies rely on positional data, often transformed into spatial grids or differential coordinates. Table 7 summarizes which models use speed, course, or both from 2019 to 2025. Speed is used in 12 papers, the course in 4, and they overlap in 11. Their use has increased in recent years, improving accuracy in dynamic routing.

Figure 2 presents a timeline of papers using speed and course features and a categorization based on whether they use speed, course, or both. The number of models integrating

Table 6 Papers using contextual and environmental datasets with data types, sources, the place and time of data gathering, and approximate size

Citation	Description
Donandt et al. [72]	Type: river curvature (radii), Source: BAW, Place: Danube
Mehri et al. [21]	Type: wave (height, direction, and wavelength), water depth,
	wind (speed and direction), temperature, humidity, precipitation,
	atmospheric pressure, and visibility, Source: SHOM-IFREMER,
	English Channel (45° N to 51° N and 10° W to 0° W), Feb. 2016,
	43,206 grid sampling points and 16 weather stations
Bi et al. [98]	Type: wave (height and period), wind (speed and direction), and
	tide (direction and speed), Place: Jiangsu, Yangtze (34.40° N to
	35.47° N and 119.17° E to 120.41° E), Time: Jan. to Dec. 2022
Wang et al. [105]	Type: wave height, wind (speed and direction), and temperature,
	Source: ECMWF and World Weather Online,
	Place: 55.5° N to 58° N and 13° W to 10.3° W, Time:
	02.01.–24.02.2024, 1,153,654 records (timestamps every 3 h)
Zhou et al. [3]	Type: wave height, wind speed, water current, and OMAOD550,
	Source: CMEMS and the ERA5 dataset of ECMWF,
	Kattegat and the Gulf of Mexico, July 2022 and 28.09.2022

Table 7 Papers using speed, course, or both variables from 2019 to 2025

Citation	Speed	Course	Speed + course
Rong et al. [5]	+	-	-
Üney et al. [4]	+	-	-
Total (2019): 2	**2**	**0**	**0**
Ding et al. [73]	-	-	+
Karataş et al. [60]	+	-	-
Suo et al. [6]	-	-	+
Wang et al. [19]	+	-	-
Total (2020): 4	**2**	**0**	**2**
Anne et al. [68]	+	-	-
Zhao et al. [63]	+	-	-
Zheng et al. [79]	+	-	-
Total (2022): 3	**3**	**0**	**0**
Gao et al. [89]	-	+	-
Li et al. [83]	+	-	-
Petrovic et al. [57]	-	-	+
Wang and Xiao [90]	-	-	+
Zhang et al. [86]	-	-	+
Zhang et al. [80]	-	-	+
Zhao and Zhang [81]	+	-	-
Total (2023): 7	**2**	**1**	**4**
Bi et al. [98]	-	-	+
Li et al. [100]	+	-	-
Li et al. [107]	+	-	-
Li et al. [8]	-	+	-
Shin et al. [101]	-	-	+
Takahashi et al. [109]	-	+	-
Zhang et al. [95]	-	+	-
Zhou et al. [99]	-	-	+
Total (2024): 8	**2**	**3**	**3**
Drapier et al. [106]	-	-	+
Liu et al. [2]	+	-	-
Zhou et al. [3]	-	-	+
Total (2025): 3	**1**	**0**	**2**
Total (2019–2025): 27	**12**	**4**	**11**

both features is increasing. The dual use of speed and course has become dominant by 2024, reflecting the increased complexity of models and richer feature inputs.

Üney et al. [4] construct a stochastic kinematics model based on an OU process, which incorporates speed. Rong et al. [5] decompose trajectories into lateral and longitudinal components, predicting position probability distributions using a GP and historical acceleration statistics. Petrovic et al. [57] improve prediction accuracy by using speed and course to estimate velocities along both axes and by modeling the complex relationship between heading and trajectory. However, there are fewer examples of directly using speed and heading estimates as output.

3 Methodology

3.1 Statistical, clustering, or graph-based methods

Table 8 tracks Bayes, Markov, DBSCAN, and graph models. Graph methods are the most prevalent, with 14 examples, followed by DBSCAN, with 8 papers. Bayesian and Markov models dominate early studies, with 4 and 3 studies, respectively, for each topic.

Clustering methods [20] and statistical methods [5] form the backbone of early maritime forecasting [15] because they are interpretable and computationally efficient. Traditional

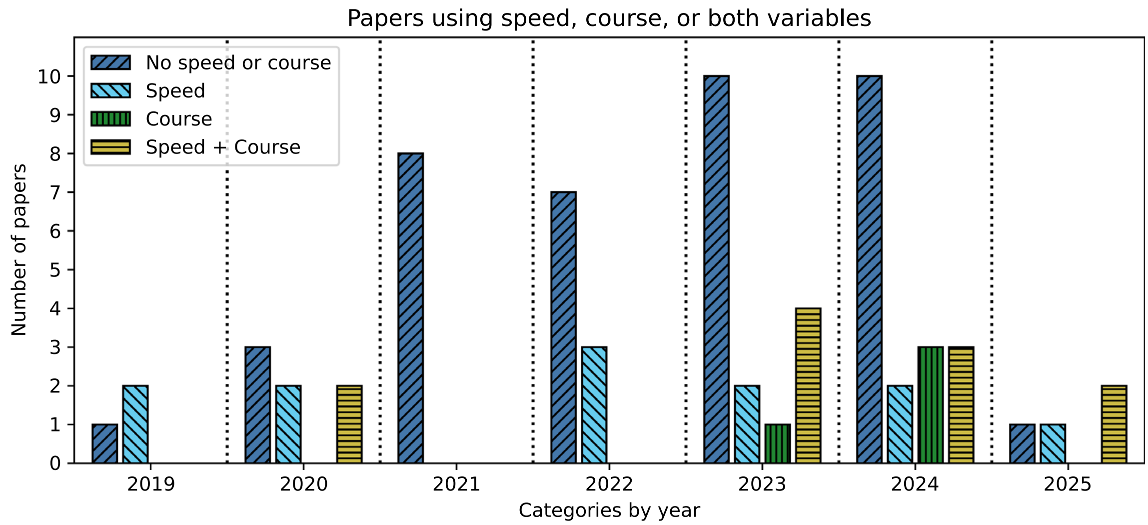

Fig. 2 Timeline for papers using speed, or course

statistical approaches are often favored as baselines [104] for vessel trajectory forecasting due to their interpretability and relatively low computational cost.

Bayesian models [88] employing an OU [4] or a GP [5] approach produce probabilistic forecasts and uncertainty quantification.

Üney et al. [4] use a hierarchical stochastic model with change points and Bayesian inference with Ornstein–Uhlenbeck processes to model stochastic vessel dynamics for long-term predictions. Rong et al. [5] apply Bayesian estimation to probabilistic path forecasting, improving upon traditional filtering techniques by modeling trajectory uncertainty using Gaussian Process Regression (GPR) for lateral motion and acceleration, and modeling longitudinal motion.

Markov chains [104] model vessel behavior as transitions between discrete states [55], showing good results for short-term prediction. Other papers by Chondrodima et al. [17] and Zhang et al. [80] integrated a Hidden Markov Model (HMM) for modeling vessel behavior as transitions between discrete states, often for short-term prediction.

Figure 3 shows a timeline for statistical, clustering, or graph-based methods and tracks classical methods over time. The number of Bayesian approaches is very low in general, with one paper in 2019 [5] and one in 2023 [88] using a purely Bayesian method, and one combining a graph-based approach [4]. The findings are similar for Markov chain approaches, with one paper in 2024 [104], and three in 2023 [17, 55, 80].

Graph-based methods [91] are among the most promising innovations [63]. Spatiotemporal graph-based models [61] segment routes and identify anomalous patterns [13]. Üney et al. [4] apply spatial graphs to encode vessel positions. Jiang et al. [14] propose STMGF-Net, which captures dynamic interaction relationships among vessels. Graph-based meth-

Table 8 Papers using statistical, clustering, or graph-based methods from 2019 to 2025

Citation	Bayes	Markov	DBSCAN	Graph
Li et al. [20]	-	-	+	-
Rong et al. [5]	+	-	-	-
Üney et al. [4]	+	-	-	+
Total (2019): 3	**2**	**0**	**1**	**1**
Murray and Perera [70]	-	-	+	-
Suo et al. [6]	-	-	+	-
Wang et al. [19]	-	-	-	+
Total (2020): 3	**0**	**0**	**2**	**1**
Mehri et al. [76]	-	-	-	+
Total (2021): 1	**0**	**0**	**0**	**1**
Anne et al. [68]	-	-	+	-
Liang et al. [61]	-	-	-	+
Liu et al. [13]	-	-	-	+
Zhang et al. [16]	-	-	+	-
Zhao et al. [63]	-	-	-	+
Total (2022): 5	**0**	**0**	**2**	**3**
Capobianco et al. [88]	+	-	-	-
Chondrodima et al. [17]	-	+	-	-
Hao et al. [12]	-	-	-	+
Jurkus et al. [22]	-	-	-	+
Xiao et al. [55]	-	+	-	-
Zhang et al. [80]	-	+	-	-
Zhao et al. [91]	-	-	-	+
Total (2023): 7	**1**	**3**	**0**	**3**
Bi et al. [98]	-	-	-	+
Gao et al. [7]	-	-	+	-
Han et al. [104]	-	+	-	-

Table 8 continued

Citation	Bayes	Markov	DBSCAN	Graph
Jiang et al. [15]	-	-	+	-
Jiang et al. [14]	-	-	-	+
Shin et al. [101]	-	-	-	+
Xue et al. [9]	-	-	+	-
Zhou et al. [99]	-	-	-	+
Total (2024): 8	**0**	**1**	**3**	**4**
Zhou et al. [3]	-	-	-	+
Total (2025): 1	**0**	**0**	**0**	**1**
Total (2019–2025): 28	**3**	**4**	**8**	**14**

ods outperform traditional sequence models (LSTM or GRU) by better modeling environmental and behavioral context. In comparison, single-graph models, such as GAT [12], offer fewer representational capacities than their multi-graph counterparts.

Figure 4 represents pie charts of speed and course features integrated into classical methods, combining feature use and model type. Graph-based clustering is often used without speed and course inputs, as we have found that 7 out of 13 papers with graph structures used only position as input. The findings are similar for DBSCAN, as 6 out of 8 papers use neither speed nor course. For papers that do not use statistical, clustering, or graph-based methods, only 7 use speed, 4 use course, and 5 use both. Only one out of 4 Markov chain papers uses speed and course [80].

Clustering methods, such as DBSCAN [70], are employed for clustering trajectories and identifying traffic lanes [20] and port approach paths [15]. Although they are limited in their ability to capture long-term dependencies and often fail and react poorly to noisy data under highly dynamic or non-linear conditions, these methods are foundational and often serve as components in hybrid models. DBSCAN clustering remains popular in port detection and traffic lane segmentation.

Clustering use use is evident in Suo et al. [6], Anne et al. [68], and Zhang et al. [16], and has been expanded for risk assessment and operational routing by Gao et al. [7].

3.2 Recurrent neural networks

Table 9 presents a breakdown of RNN, GRU, LSTM, and hybrid model use from 2019 to 2025. LSTM is the most widely used model variant in 28 papers, with GRU adoption increasing after 2022. There are 8 LSTM papers in 2023, and 3 using GRU and LSTM approaches [22, 83, 93], with 4 more LSTM studies and 2 using GRU and LSTM in 2024 [9, 97]. In 2022, there were 5 LSTM papers, and 6 in 2021, with only 3 and 1 in 2020 [60, 73, 77] and 2019 [20], respectively. In 2020, 2 additional papers used GRU and LSTM approaches [6, 10]. Purely GRU approaches are employed in two papers in 2023 [12, 84] and one in 2021 [18], and the most recent examples are two papers in 2024 [98, 107].

RNN structures, especially LSTM and GRU variants [18], have become standard in sequence-based trajectory prediction, owing to their ability to learn temporal dependencies in vessel movements. They model temporal dependencies effectively and can be enriched and extended to construct hybrid models. Vanilla RNN architectures [67] are simpler but still perform well on clean data and engineered features.

Figure 5 demonstrates the timeline for papers using methods with GRU, LSTM, and RNN architectures [67]. GRU and LSTM combinations [6, 10] rise significantly in 2023 [22, 83, 93] and 2024 [9, 97], with improved performance in complex forecasting scenarios. The number of LSTM-based

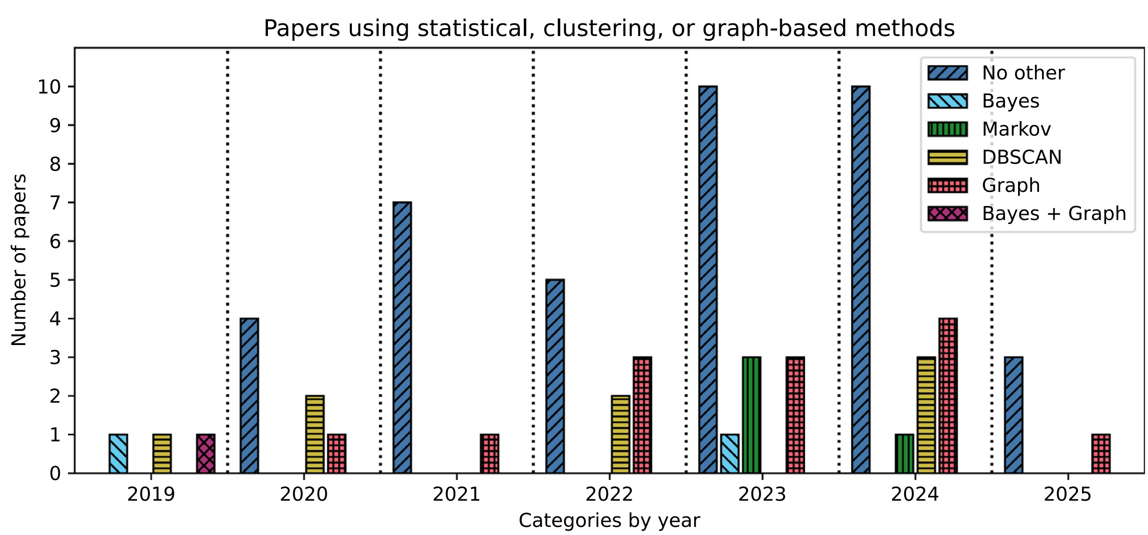

Fig. 3 Timeline for papers using statistical, clustering, or graph-based methods

Fig. 4 Pie charts for papers using statistical, clustering, or graph-based methods, and speed, or course

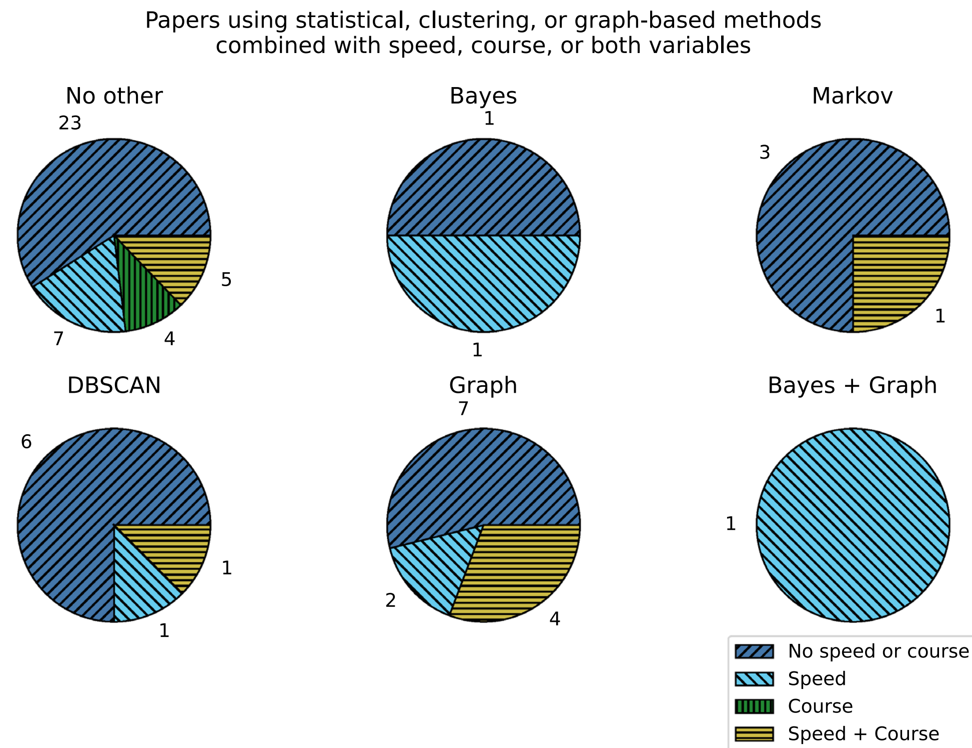

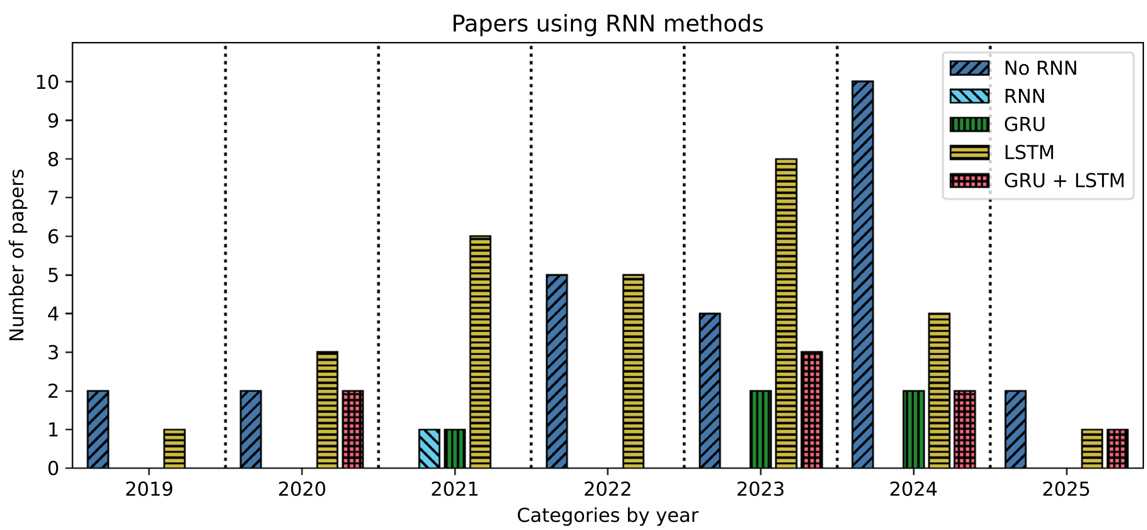

Fig. 5 Timeline for papers using RNN methods

manuscripts rises from 5 in 2022 to 8 in 2023, slightly dropping to 4 in 2024.

Pie charts for RNN models that combine speed and course as inputs are shown in Fig. 6 and indicate that RNN architectures are increasingly paired with these features, reflecting their suitability for continuous dynamic forecasting. Out of 5 GRU-only papers, 3 do not use speed or course [12, 18, 84], and 5 out of 8 GRU and LSTM papers follow that approach. The findings are similar for pure LSTM architectures, with 16 out of 28 that do not rely on speed or course. For papers with no RNN approaches, 15 out of 25 do not exploit speed or course. Three papers use no RNN methods and course [8, 89, 95], and three use no RNN methods and speed and course [3, 86, 101]. One RNN paper uses neither speed nor course [67]. One GRU paper [107] and one GRU-LSTM paper [83] use speed, and one LSTM paper uses course [109]. A GRU approach [98] and two GRU and LSTM approaches [6, 106] use speed and course.

Zhu [67] implements an RNN using AIS input vectors, whereas others, including Capobianco et al. [88], extend

Table 9 Papers using RNN methods from 2019 to 2025

Citation	RNN	GRU	LSTM	GRU + LSTM
Li et al. [20]	-	-	+	-
Total (2019): 1	**0**	**0**	**1**	**0**
Ding et al. [73]	-	-	+	-
Karataş et al. [60]	-	-	+	-
Suo et al. [6]	-	-	-	+
You et al. [10]	-	-	-	+
Zhang et al. [77]	-	-	+	-
Total (2020): 5	**0**	**0**	**3**	**2**
Gao et al. [62]	-	-	+	-
Liu et al. [66]	-	-	+	-
Lu et al. [74]	-	-	+	-
Mehri et al. [76]	-	-	+	-
Pan et al. [64]	-	-	+	-
Zhang et al. [18]	-	+	-	-
Zhang et al. [75]	-	-	+	-
Zhu [67]	+	-	-	-
Total (2021): 8	**1**	**1**	**6**	**0**
Anne et al. [68]	-	-	+	-
Donandt et al. [72]	-	-	+	-
Sørensen et al. [71]	-	-	+	-
Yang et al. [69]	-	-	+	-
Zhao et al. [63]	-	-	+	-
Total (2022): 5	**0**	**0**	**5**	**0**
Cao et al. [84]	-	+	-	-
Capobianco et al. [88]	-	-	+	-
Chondrodima et al. [17]	-	-	+	-
Hao et al. [12]	-	+	-	-
Jurkus et al. [22]	-	-	-	+
Li et al. [83]	-	-	-	+
Mehri et al. [21]	-	-	+	-
Petrovic et al. [57]	-	-	+	-
Spadon et al. [93]	-	-	-	+
Wang and Xiao [90]	-	-	+	-
Zhang et al. [80]	-	-	+	-
Zhao et al. [91]	-	-	+	-
Zhao and Zhang [81]	-	-	+	-
Total (2023): 13	**0**	**2**	**8**	**3**
Bi et al. [98]	-	+	-	-
Dong et al. [97]	-	-	-	+
Li et al. [100]	-	-	+	-
Li et al. [107]	-	+	-	-
Takahashi et al. [109]	-	-	+	-
Xiao et al. [96]	-	-	+	-
Xue et al. [9]	-	-	-	+
Zhou et al. [99]	-	-	+	-
Total (2024): 8	**0**	**2**	**4**	**2**
Drapier et al. [106]	-	-	-	+
Liu et al. [2]	-	-	+	-
Total (2025): 2	**0**	**0**	**1**	**1**
Total (2019–2025): 42	**1**	**5**	**28**	**8**

RNN models with Bayesian dropout to model uncertainty. LSTM variants [91] dominate trajectory forecasting in the observed timeframe, as shown by Zhou et al. [99] and Zhao et al. [63]. Jurkus et al. [22] combine bidirectional LSTM layers with Cartesian velocity inputs, showing improved handling of circular course data. While basic and conventional RNN models are reliable for short- and medium-term forecasting, they struggle with long-term prediction and may accumulate errors [104].

However, with several enhancements, such as clustering [6] and attention mechanisms [10], recent studies have used LSTM and GRU [107] networks for sequence modeling with speed, heading, and position data for mid- to long-term forecasting. Innovative convolution [93, 97, 98], encoder-decoder, attention [84], and Transformer [9, 106] architectures ensure that the basic area of DL remains a dominant approach. These models accommodate non-linear motion, irregular time intervals, and contextual patterns. Bidirectional RNN [12, 83] models that process sequences forward and backward can significantly improve performance. Preprocessing techniques, such as position offset normalization or feature engineering, including converting heading into Cartesian vectors [22], enhance model learning. Based on the preprocessing of AIS data, Zhu [67] built an RNN model to forecast ship positions.

Pie charts for RNN models combined with classical models in Fig. 7 show that RNN models can be enhanced with clustering, graph-based structures, Bayesian, and Markov chains. There is one paper using a Bayesian model, and no RNN [5], and one using Bayes and graph-based approaches with no RNN [4]. Two papers use Markov models without an RNN [55, 104], and one paper uses an RNN model and no clustering, graph-based structures, Bayesian approaches, or Markov chains [67]. There are three GRU papers that do not use clustering, graph models, Bayes, or Markov models [18, 84, 107], and two that use GRU and graph techniques [12, 98]. One paper uses an LSTM Bayes hybrid [88], and two use LSTM and Markov chains [17, 80]. Two papers combine LSTM and DBSCAN [20, 68], and two more use GRU,

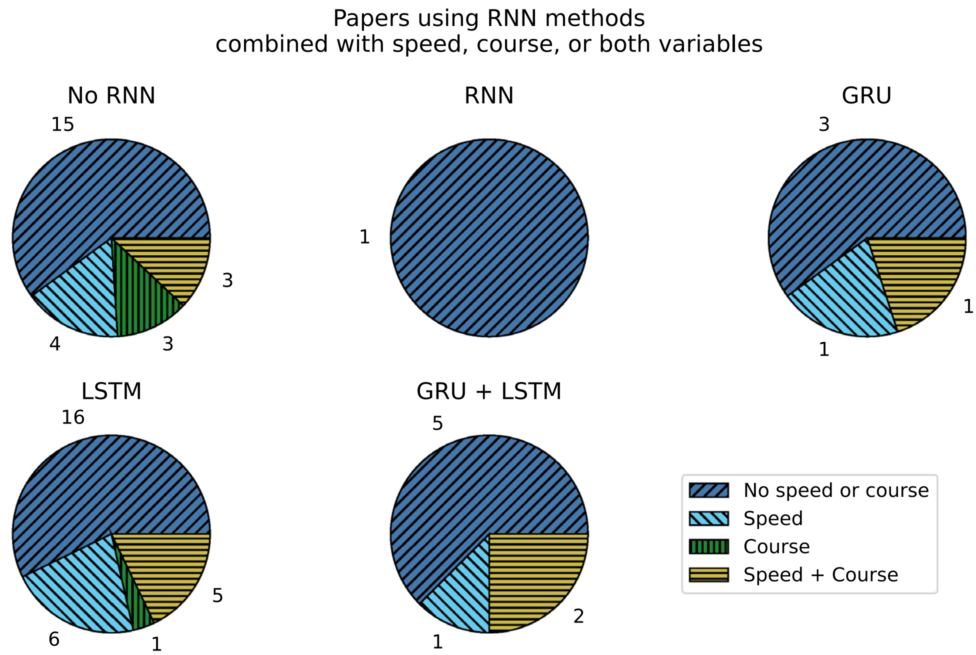

Fig. 6 Pie charts for papers using RNN methods, and speed, or course

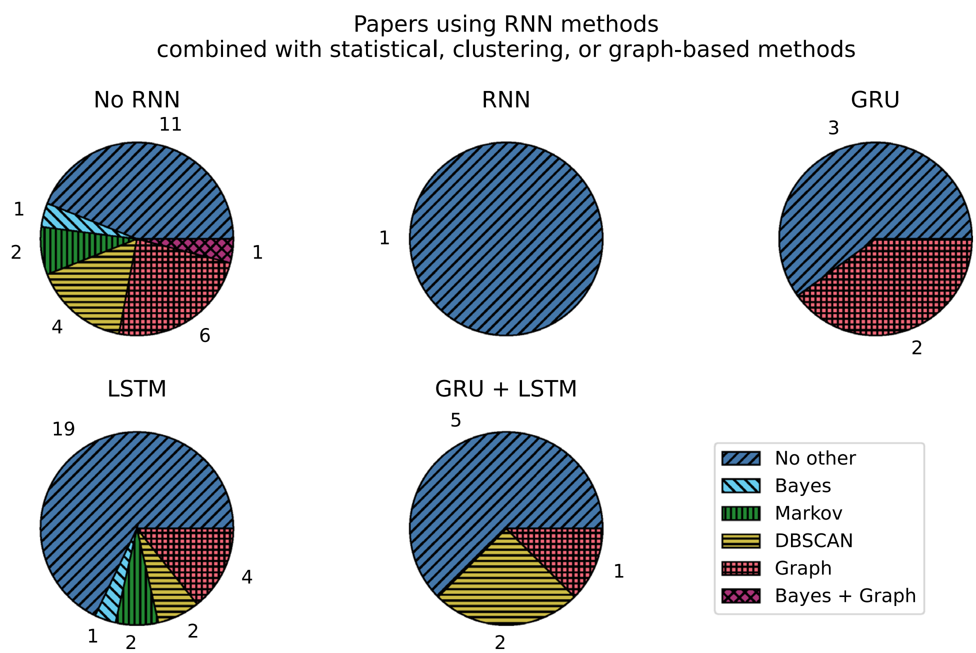

Fig. 7 Pie charts for papers using RNN methods, and statistical, clustering, or graph-based methods

LSTM, and DBSCAN [6, 9]. Finally, one paper uses GRU, LSTM, and graph approaches [22].

The summarized findings indicate that there are 11 papers that use no RNN approaches and no clustering, graph-based structures, Bayesian approaches, or Markov chains, and 19 more papers that use LSTM without any of the other listed supplementary approaches. This highlights the need for more hybrid models in future, as 4 models use DBSCAN and no RNN, and 6 use graph-based approaches with no RNN, compared with only 4 models with LSTM and graph-based approaches.

3.3 Deep learning models

Table 10 captures the use of attention, bidirectional layers, CNN models, and autoencoders from 2020 to 2025. Attention models have dominated recent years with 24 papers, confirming a shift toward foundation forecasting models and hybrid attention structures. The strong presence of both CNN and autoencoder models, with 15 and 10 papers related to these concepts, respectively, proves that these architectures are still relevant, especially in hybrid configurations. The number of CNN models shifted from 2 in 2021 [18, 74] to 5 in 2022,

Table 10 Papers using autoencoders, attention, bidirectional layers, and CNN methods from 2020 to 2025

Citation	Autoencoder	Attention	Bidirectional	CNN
Murray and Perera [70]	+	-	-	-
Wang et al. [19]	-	+	-	-
You et al. [10]	-	+	-	-
Total (2020): 3	**1**	**2**	**0**	**0**
Gao et al. [62]	-	+	-	-
Lu et al. [74]	-	+	-	+
Zhang et al. [18]	-	+	-	+
Zhang et al. [75]	-	+	+	-
Total (2021): 4	**0**	**4**	**1**	**2**
Anne et al. [68]	+	-	-	-
Liang et al. [61]	-	-	-	+
Liu et al. [13]	-	+	-	+
Sørensen et al. [71]	-	+	+	-
Yang et al. [69]	-	+	+	-
Zhang et al. [16]	-	-	-	+
Zhao et al. [65]	-	+	-	-
Zhao et al. [63]	-	+	-	+
Zheng et al. [79]	-	-	-	+
Total (2022): 9	**1**	**5**	**2**	**5**
Cao et al. [84]	-	+	-	-
Capobianco et al. [88]	+	-	-	-
Gao et al. [89]	+	-	-	-
Hao et al. [12]	-	+	+	-
Jurkus et al. [22]	+	-	+	-
Li et al. [83]	-	-	+	-
Spadon et al. [93]	-	-	-	+
Wang and Xiao [90]	+	-	-	+
Xiao et al. [55]	+	-	+	-
Zhang et al. [86]	-	+	-	-
Zhao et al. [91]	-	+	-	-
Total (2023): 11	**5**	**4**	**4**	**2**
Bi et al. [98]	-	+	-	+
Dong et al. [97]	-	+	-	+
Han et al. [104]	+	-	-	-
Jiang et al. [15]	-	+	-	-
Jiang et al. [14]	-	+	-	+
Li et al. [100]	-	+	-	-
Li et al. [107]	-	+	-	+
Shin et al. [101]	+	-	-	+
Spadon et al. [102]	+	-	-	-
Zhang et al. [11]	-	-	+	-
Zhang et al. [95]	-	+	-	-
Zhou et al. [99]	-	+	-	-
Total (2024): 12	**3**	**8**	**1**	**5**
Zhou et al. [3]	-	+	-	+
Total (2025): 1	**0**	**1**	**0**	**1**
Total (2020–2025): 40	**10**	**24**	**8**	**15**

then to 2 in 2023 [90, 93], and again to 5 in 2024, ending with 1 model in 2025 [3]. There was one autoencoder in 2020 [70], one in 2022 [68], five in 2023, and three more in 2024 [101, 102, 104].

Table 11 focuses on the Transformer architecture from 2022 to 2025, while including one paper that uses a KAN to highlight the latest developments in explainable models [2]. Following closely on the more general attention concept, the 13 papers using transformers confirm that a paradigm shift is underway.

DL approaches now dominate state-of-the-art prediction models. Transformers, such as the Trajectory Automatic Identification System Transformer (TrAISformer) [8] and the Gated Recurrent Unit Transformer (G-Trans) [9], outperform RNN architectures by capturing long-range dependencies via self-attention (SA). They are useful in noisy, sparse, or multi-modal data environments.

Murray and Perera [70] used a dual linear autoencoder and generative models to generalize trajectory patterns under uncertainty. Attention models were introduced into maritime forecasting, namely the bidirectional Long Short-Term Memory (Bi-LSTM) [10] and Sequence-to-Sequence (Seq2Seq) architecture [10], to handle bidirectional dependencies [10] and long-term sequence modeling [10], enabling long-term, multi-feature learning. Transformer variants by Zhang et al. [11] and Xiao et al. [55] outperform baselines in trajectory smoothness and error reduction [8]. TrAISformer [8] is a Transformer-based model introduced to capture multi-modal trajectory distributions and waypoint transitions with excellent performance, benchmarking highly against other methods and capturing long-range dependencies using Multi-head Attention (MHA), outperforming LSTM and Seq2Seq on multimodal trajectory prediction tasks by using the full AIS context in sequence modeling and capturing long-range dependencies via SA. Models, such as TrAISformer [8] and G-Trans [9], deliver state-of-the-art performance, especially in long-sequence, noisy, and multimodal data scenarios by using positional encoding, MHA, and sequence-wide context. Despite the best performance, concerns about model complexity remain.

Figure 8 contains a timeline for DL methods by year. Bidirectional Transformer architectures [11, 83] or CNN and attention hybrids [97, 107] are particularly prevalent from 2023 onward [14, 98]. The timeline shows that there were 3

Table 11 Papers using Transformer and KAN methods from 2022 to 2025

Citation	Transformer	KAN
Donandt et al. [72]	+	-
Total (2022): 1	**1**	**0**
Li et al. [83]	+	-
Zhang et al. [82]	+	-
Total (2023): 2	**2**	**0**
Gao et al. [7]	+	-
Li et al. [8]	+	-
Nguyen and Fablet [108]	+	-
Takahashi et al. [109]	+	-
Xiao et al. [96]	+	-
Xue et al. [9]	+	-
Zhang et al. [11]	+	-
Total (2024): 7	**7**	**0**
Drapier et al. [106]	+	-
Liu et al. [2]	-	+
Wang et al. [105]	+	-
Zhou et al. [3]	+	-
Total (2025): 4	**3**	**1**
Total (2022–2025): 14	**13**	**1**

pure CNNs in 2022 [16, 61, 79] and 1 in 2023 [93], and 2 attention-CNN hybrids in 2021 [18, 74] and 2022 [13, 63] each, peaking at 4 such models in 2024. There is one attention-bidirectional approach in 2021 [75], two more in 2022 [69, 71], and one more in 2023 [12].

Figure 9 shows pie charts for deep learning methods by feature and method overlap. DL models increasingly incorporate multi-feature inputs.

One model uses an autoencoder with speed as input [68], and another uses course [89]. There are 2 models with speed and attention [19, 100], and 1 with attention and course [95]. Two additional approaches highlight speed, course, and attention [86, 99], and two others use a Transformer and the course variable [8, 109]. One paper combines a Transformer with speed and course [106], in contrast to three papers that use a CNN but do not incorporate speed or course [16, 61, 93].

However, one paper does supplement a CNN with speed input [79], and another approach uses speed and a KAN [2]. There are attention-CNN hybrids with speed input [63, 107], and one with speed and course as input [98]. There are two combined bidirectional and autoencoder approaches that do not use speed or course [22, 55], and one bidirectional and Transformer approach that also omits those variables [11]. On the other hand, one bidirectional and Transformer model uses speed [83], and two autoencoder-CNN hybrids use both speed and course [90, 101]. In one paper that uses attention, a Transformer, and a CNN, both speed and course input variables are introduced [3].

Figure 10 shows pie charts for DL methods merged with statistical, clustering, or graph-based methods. GNN models in STMGCN [13] and STMGF-Net [15] represent a leap in structured prediction by encoding vessel interactions as edge-weighted graphs. These systems surpass conventional RNN and CNN models in precision and generalizability, paving the way for robust spatiotemporal maritime intelligence.

One paper uses no DL and a Bayes model [5]. Two studies do not use DL but use Markov models [17, 80]. Two more works also use DBSCAN without DL [6, 20]. There is also one graph model with no DL [76], and one graph-Bayes model with no DL [4]. There are two autoencoders that do not use statistical, clustering, or graph-based methods [89, 102]. However, one autoencoder uses a Bayesian approach [88], and another uses a Markov model [104]. Continuing in this hybrid fashion, two autoencoders use DBSCAN [68, 70], and one attention mechanism is supplemented with DBSCAN [15]. There are three attention-graph hybrids [19, 91, 99], and two Transformer-DBSCAN hybrids [7, 9]. On the other hand, two CNNs do not use Bayes, Markov, graph, or DBSCAN approaches [79, 93]. In contrast, one CNN uses DBSCAN [16], while another adopts a graph-based approach [61]. The reviewed KAN model does not use any graph-based, Bayesian, Markov, or clustering techniques [2]. There are three attention-bidirectional hybrids that also omit these supplemental approaches [69, 71, 75].

On a more positive note, one attention-bidirectional hybrid uses a graph-based approach [12], while an alternative autoencoder-bidirectional model is supplemented with a Markov model [55]. A different autoencoder-bidirectional hybrid also uses a graph model [22], in contrast to two Transformer-bidirectional approaches that do not use any statistical, clustering, or graph-based techniques [11, 83]. There is also an autoencoder-CNN combination that overlooks these additions [90], but another autoencoder-CNN approach uses a graph-based approach [101]. A single paper found that attention, a Transformer, and a CNN were used in tandem with graph-based techniques [3], demonstrating that a novel hybrid modeling approach can yield results.

Figure 11 shows pie charts for hybrid DL methods using RNN models with attention, Transformer architectures, bidirectional layers, or convolution. Hybrid approaches incorporating CNN models for spatial encoding, such as CNN-LSTM models [74], the CNN LSTM Squeeze-and-Excitation (CNN-LSTM-SE) [90], and CNN Mish Temporal Attention Bidirectional GRU (CNN-MTABiGRU) [97], further enhance robustness in complex geographies by integrating CNN architectures for spatial feature extraction and RNN structures for temporal modeling and high adaptability. Two papers do not use RNNs or DL [4, 5], and three more

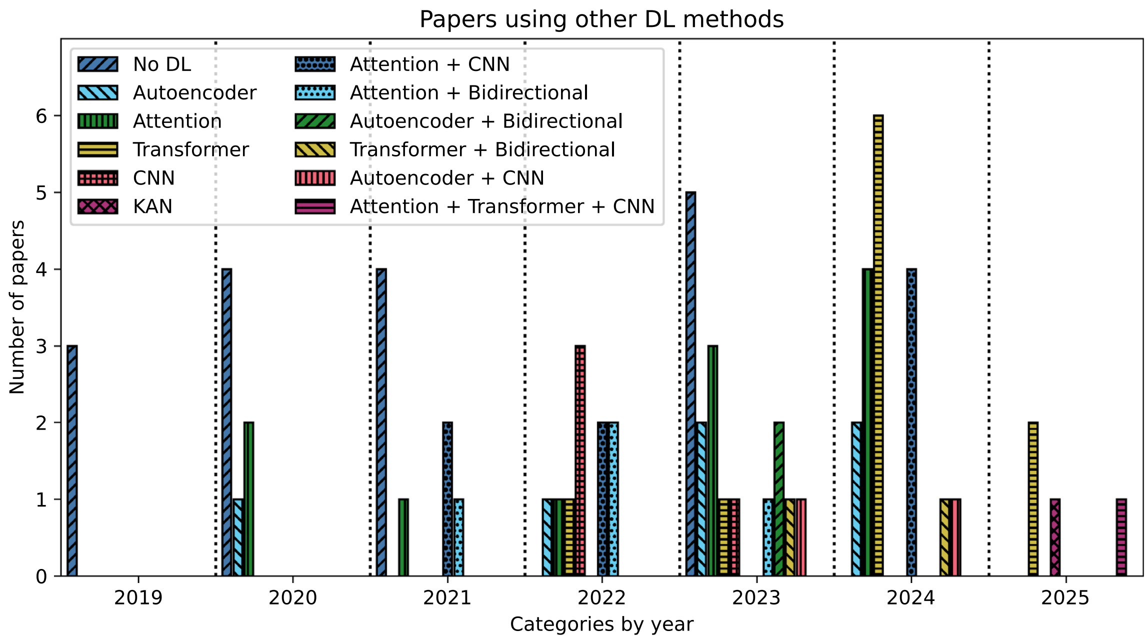

Fig. 8 Timeline for papers using other DL methods

Fig. 9 Pie charts for papers using other DL methods, and speed, or course

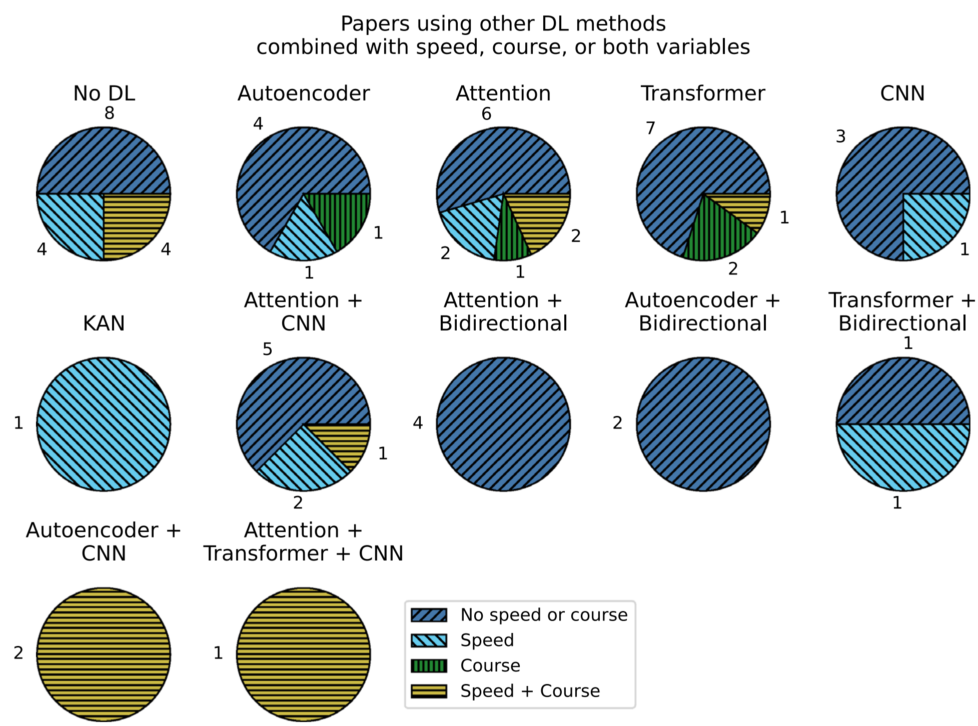

do not use RNNs, but rely on CNNs instead [16, 61, 79], so more combined approaches are needed.

Two papers do not use RNNs but instead employ attention and CNNs [13, 14]. One paper without RNNs uses an autoencoder and a bidirectional approach [55], and another uses a Transformer with a bidirectional approach [11]. Another paper uses an autoencoder and a CNN without RNNs [101], and another uses attention, a Transformer, and a CNN instead [3]. Moving on to RNN papers, one does not use DL [67], while another uses a GRU with attention [84]. Three more papers use a GRU, attention, and a CNN [18, 98, 107], and one uses a GRU, attention, and a bidirectional approach [12]. There are two LSTM autoencoders [68, 88] and three LSTM Transformers [72, 96, 109]. One paper uses LSTMs and a KAN [2], and two additional approaches combine an LSTM with attention and a CNN [63, 74]. Three papers use LSTMs,

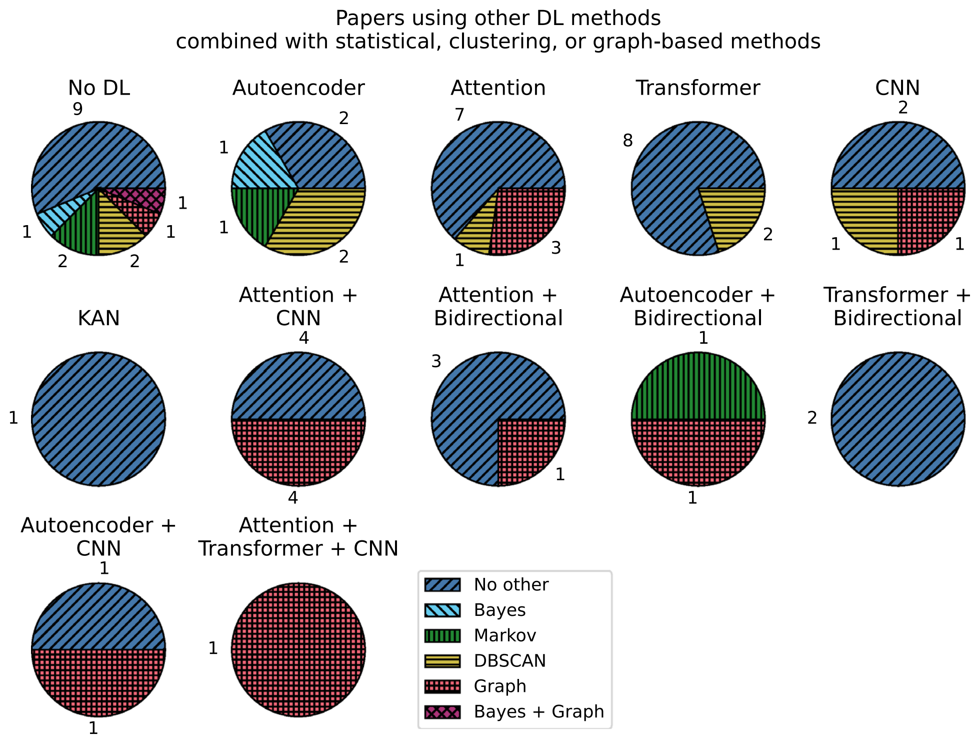

Fig. 10 Pie charts for papers using other DL methods, and statistical, clustering, or graph-based methods

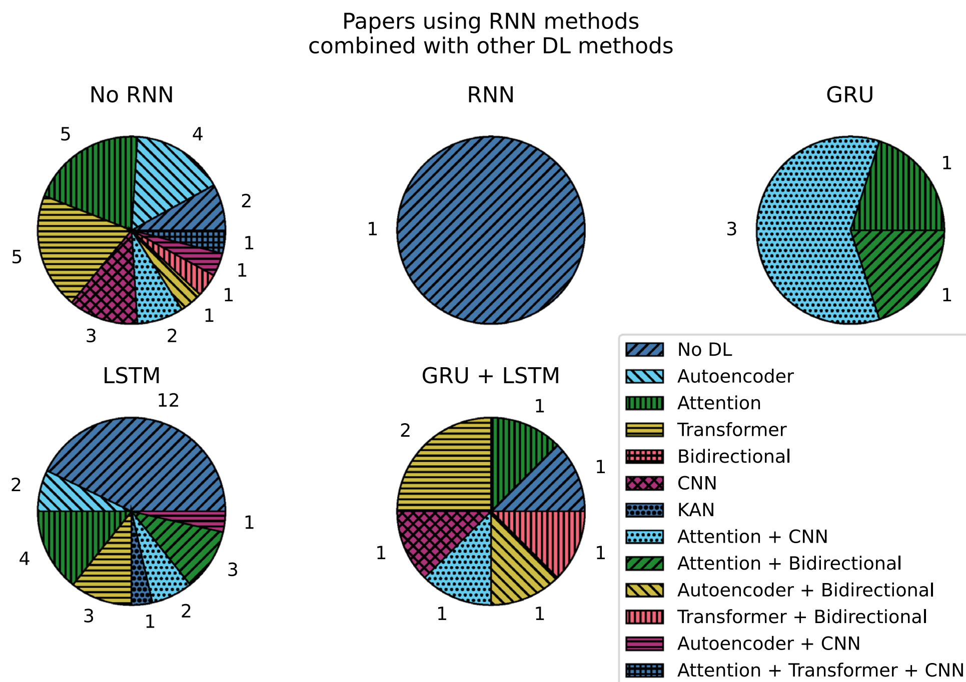

Fig. 11 Pie charts for papers using RNN methods, and other DL methods

attention, and a bidirectional model [69, 71, 75], and one LSTM uses an autoencoder and a CNN [90]. There is one GRU-LSTM hybrid with no DL [6], and one with attention [10]. Two more GRU-LSTM hybrids use a Transformer [9, 106], while one relies on a CNN [93]. The remaining GRU-LSTM approaches are combined with attention and a CNN [97], an autoencoder and a bidirectional model [22], or a Transformer and a bidirectional model [83]. However, these models incur higher computational costs and may require substantial resources and large datasets for training. Ongoing research should address generalization, interpretability [3], and performance under limited data availability.

4 Discussion

While recent advancements in data-driven vessel trajectory forecasting have led to significant performance gains, several key limitations persist that affect real-world deployment and reliability.

Computational complexity and deployment constraints plague many of the most accurate models, particularly those based on DL architectures such as LSTM, GRU, and Transformer variants. These architectures require considerable computational resources for both training and inference. These models often require a high-memory Graphics Processing Unit (GPU), large datasets, and extensive tuning, which may be infeasible for deployment on edge devices or systems with constrained computational capacity, such as onboard ship equipment or port monitoring terminals in developing regions. Moreover, real-time trajectory forecasting at scale necessitates not only efficient inference but also robust data pipelines and low-latency processing, which remain challenging under operational constraints.

The AIS data, while foundational to most trajectory forecasting systems, are susceptible to a range of reliability and integrity issues. Increasing reports of AIS spoofing, where vessels transmit false location or identity data, pose serious risks to the integrity of model inputs. Such spoofing may be used to obscure vessel movements for strategic, commercial, or illicit purposes, as seen in cases involving smuggling, illegal fishing, or military deception, such as the concealment of trajectories by hostile nations. Furthermore, AIS jamming, OOS, and deliberate signal suppression by so-called dark ships introduce further uncertainty into the data stream. These behaviors not only reduce forecasting accuracy but also necessitate the development of robust anomaly-detection and data-validation techniques, ideally using cross-modal verification with satellite, radar, or sensor-fusion systems.

Another obstacle lies in the limited generalizability and dataset bias of models trained on geographically or temporally narrow datasets. Many current approaches use AIS data limited to specific regions or vessel types, which may not capture the full variability of global maritime traffic. This raises concerns about model transferability and adaptability in unseen operational contexts or under changing environmental and behavioral conditions.

Addressing these limitations is essential for building forecasting systems that are not only accurate under ideal conditions but also resilient, efficient, and trustworthy in operational maritime environments.

4.1 The intended purposes of trajectory forecasting across the surveyed works

As the forecasts generated by various models may be used for a wide variety of purposes, not all of which should be grouped together, we begin the discussion by categorizing the papers by broad general areas (anomaly detection (AD), collision avoidance (CA), and traffic management (TM)) and providing a brief description for each paper. Table 12 contains this overview from 2019–2022, which will be continued in Table 13 for subsequent years. In 2019, one paper covers the combined topics of anomaly detection, collision avoidance, and traffic management [20], one is categorized under both anomaly detection and traffic management [5], and one is intended solely for traffic management [4].

There are two papers on collision avoidance from 2020 [10, 70] in Table 12. One combines it with traffic management [73], and four deal only with traffic management.

There are also two papers on collision avoidance from 2021 [62, 67] and one paper that merges collision avoidance and traffic management [66], with five more on traffic management only.

Three papers in 2022 merge collision avoidance with traffic management [13, 69, 71]. Six 2022 works address only traffic management, such as the approach using the Density-Based Spatial Clustering of Applications with Noise Temporal Convolutional Network (D-TCN) [16] or the paper using a k-hop Graph Convolutional Network (GCN) and LSTM (k-GCN-LSTM). Only one 2022 paper focuses on anomaly detection as the sole objective [68].

Table 13 continues the paper classification by purpose for 2023–2025. Two papers deal with collision avoidance in 2023 [86, 88], and one paper deals with anomaly detection, collision avoidance, and traffic management [83]. Six additional papers focused solely on traffic management, and eight combined collision avoidance and traffic management, including the Encoder Decoder Attention (EDA) GRU approach [84].

One paper in 2024 also highlighted all three application areas (anomaly detection, collision avoidance, and traffic management) [107], whereas 7 papers in 2024 exclusively address traffic management. Five 2024 studies focused solely on collision avoidance, and five more tackled both collision avoidance and traffic management.

Two 2025 works [105, 106] state the intended purpose as traffic management, including one utilizing the H3 index and CLM [106]. One 2025 paper is placed in the domain of collision avoidance [2], and one at the intersection of collision avoidance and traffic management [3].

Only three papers in total touch upon anomaly detection, collision avoidance, and traffic management [20, 83, 107]. Only one paper combines anomaly detection and traffic management [5], and one is placed in the subject area of pure anomaly detection [68]. There are 33 papers classified as traffic management works [12], since trajectory prediction has its main use cases in ship arrival time prediction and port scheduling. The second-largest area, with 17 papers, is collision avoidance and traffic management [55], in which ships

Table 12 The intended purposes (anomaly detection (AD), collision avoidance (CA), and traffic management (TM)) of trajectory forecasting (2019–2022)

Description
Li et al. [20]: AD/CA/TM: Long-term prediction using DBSCAN and LSTM networks
Rong et al. [5]: AD/TM: Detect abnormal ship behaviors and predict trajectory uncertainty using probabilistic bounds based on a GP model
Üney et al. [4]: TM: Long-term forecast (hierarchical generative model/OU processes)
Ding et al. [73]: CA/TM: Multidimensional and long-time vessel trajectory prediction
Karataş et al. [60]: TM: Next position, arrival time, and port prediction
Murray and Perera [70]: CA: Vessel trajectory prediction
Suo et al. [6]: TM: Ship trajectory prediction using GRU and DBSCAN
Wang et al. [19]: TM: Movement detection and prediction in remote sensing videos
You et al. [10]: CA: Short-term vessel trajectory prediction
Zhang et al. [77]: TM: Ship trajectory prediction
Gao et al. [62]: CA: Multi-step ship trajectory prediction
Liu et al. [66]: CA/TM: Vessel trajectory prediction
Lu et al. [74]: TM: Ship trajectory prediction
Mehri et al. [76]: TM: Vessel movement prediction
Pan et al. [64]: TM: Predict arrival time and reduce uncertainty for smart ports
Zhang et al. [18]: TM: Predict broken trajectories in strong clutter (HF radar data)
Zhang et al. [75]: TM: Ship trajectory prediction
Zhu [67]: CA: Short-term trajectory prediction
Anne et al. [68]: AD: Predict ship trajectory using historical AIS data to determine the trajectory of ships that turn off AIS and identify anomalies
Donandt et al. [72]: TM: Short-term inland vessel trajectory prediction
Liang et al. [61]: TM: Accurate/robust fine-grained traffic flow prediction (STMGCN)
Liu et al. [13]: CA/TM: Vessel trajectory prediction using STMGCN
Sørensen et al. [71]: CA/TM: Predict probabilistic future locations of ships to assist in collision avoidance and determining the identity of dark ships using a BLSTM-MDN model
Yang et al. [69]: CA/TM: Vessel trajectory prediction using Bi-LSTM
Zhang et al. [16]: TM: D-TCN prediction for remote sensing satellite task planning
Zhao et al. [65]: TM: Ship trajectory smoothing and prediction
Zhao et al. [63]: TM: Predict ship speed using k-GCN-LSTM
Zheng et al. [79]: TM: Trajectory prediction for satellite resource scheduling and search

Table 13 The intended purposes (anomaly detection (AD), collision avoidance (CA), and traffic management (TM)) of trajectory forecasting (2023–2025)

Description
Cao et al. [84]: CA/TM: Vessel trajectory prediction (EDA GRU)
Capobianco et al. [88]: CA: Vessel trajectory prediction/uncertainty estimation
Chondrodima et al. [17]: CA/TM: Forecast locations up to 60 min in future
Gao et al. [89]: TM: Ship trajectory prediction
Hao et al. [12]: TM: Multi-ship trajectory prediction in high-density maritime traffic areas to predict future conflicts and avoid potential accidents
Jurkus et al. [22]: TM: RNN/coordinate transformation (UTM, polar, and haversine)
Li et al. [83]: AD/CA/TM: Trajectory prediction, modeling, and analysis (ML and DL)
Mehri et al. [21]: TM: A context-aware framework (CLSTM) with environmental factors
Petrovic et al. [57]: TM: Vessel classification and multivariate trajectory forecasting
Spadon et al. [93]: TM: Forecasting AIS message (latitude, longitude, COG, SOG, and delta time) from multiple vessels simultaneously under temporally noisy data
Wang and Xiao [90]: TM: Ship trajectory prediction
Xiao et al. [55]: CA/TM: Prediction for intelligent route planning and collision avoidance
Zhang et al. [82]: CA/TM: Ship trajectory prediction
Zhang et al. [86]: CA: Vessel trajectory prediction
Zhang et al. [80]: TM: Predict tugboat trajectory (HMM and K-means clustering)
Zhao et al. [91]: CA/TM: Ship trajectory prediction
Zhao and Zhang [81]: CA/TM: Ship trajectory prediction
Bi et al. [98]: CA: Ship trajectory prediction
Dong et al. [97]: CA: Ship trajectory prediction
Gao et al. [7]: CA: Regional collision risk using a predictable Transformer and DBSCAN
Han et al. [104]: CA: Short-term prediction considering interaction and uncertainty
Jiang et al. [15]: TM: Vessel trajectory prediction and route pattern classification
Jiang et al. [14]: CA/TM: Vessel trajectory forecasting
Li et al. [100]: CA/TM: Ship trajectory prediction
Li et al. [107]: AD/CA/TM: Ship trajectory prediction
Li et al. [8]: CA/TM: Spatio-temporal ship trajectory prediction
Nguyen and Fablet [108]: TM: Vessel trajectory prediction

Table 13 continued

Description
Shin et al. [101]: CA/TM: Vessel trajectory prediction
Spadon et al. [102]: CA: Multi-path long-term forecasting (vessel–whale collisions)
Takahashi et al. [109]: TM: Ship trajectory prediction
Xiao et al. [96]: TM: Ship trajectory prediction
Xue et al. [9]: CA/TM: Trajectory prediction (G-Trans with latent space clustering)
Zhang et al. [11]: TM: Vessel destination prediction
Zhang et al. [95]: TM: Long-term vessel trajectory prediction
Zhou et al. [99]: TM: Ship trajectory prediction
Drapier et al. [106]: TM: Forecasting (H3 index and Causal Language Modeling (CLM))
Liu et al. [2]: CA: Polar ship trajectory prediction
Wang et al. [105]: TM: Long-term ship trajectory prediction
Zhou et al. [3]: CA/TM: Vessel trajectory prediction under complex sea states

must act to avoid collisions with other vessels' trajectories. The area of collision avoidance in its pure form is also well represented, with 12 papers, as accidents can occur due to marine mammals, such as whales [102], or other objects in the sea, rather than other ships.

Table 14 The training time for selected papers reporting exact values

Citation	Train
Suo et al. [6]	86.99–221.24 s
You et al. [10]	167 s (Wuhan Waterway Seq2Seq)
	65 s (Chongqing Waterway Seq2Seq)
	997 s (Wuhan Waterway GRU-GRU Seq2Seq), and 261 s (Chongqing Waterway GRU-GRU Seq2Seq)
Donandt et al. [72]	7–17 min/epoch (LSTMEncDec) and approximately 2 min/epoch (Transformer)
Sørensen et al. [71]	Approximately 36 h
Gao et al. [89]	17 s/epoch (1000 epochs)
Nguyen and Fablet [108]	50 epochs
Spadon et al. [102]	3 h (15 min/epoch)
Drapier et al. [106]	175,000 steps

Table 15 The testing time for selected papers reporting exact values

Citation	Test
Murray and Perera [70]	less than 1 s
Zhao et al. [91]	0.02–0.03 ms
Nguyen and Fablet [108]	approximately 60 min for 10 days
Zhou et al. [3]	1.2812 ms

4.2 Computational time and resource requirements

When addressing the demands of complex ML and DL approaches, the first obstacle for researchers without extensive funding and resources is training time, as shown in Table 14. These approaches vary in the number of epochs, ranging from 50 [108] to 1000 [89]. Training for one epoch can take anywhere from a few seconds to a few minutes [72, 89, 102], while the entire process for all epochs is measured in hours [71, 102].

Most papers that explicitly quantify testing time do so to highlight the optimal performance of their proposed approach, as shown in Table 15. Real-time operations often require a response within one second [70], and often a millisecond-based evaluation is needed [3, 91]. Nguyen and Fablet [108] required 60 min but reported a single value for the entire 10-day test set, whereas previous studies reported values for a single response.

As most papers in Table 16 rely on heavy ML and DL models, the equipment often includes a high-performance GPU, with NVIDIA GeForce Giga Texel Shader eXtreme (GTX) and Ray Tracing Texel eXtreme (RTX) models being the most commonly used. A single unit is often insufficient, so Jurkus et al. [22] rely on the Vilnius University High-Performance Computing (HPC) and Jiang et al. [15] use a GPU server.

Most papers use an Intel i5 [21, 77, 90], i7, or i9 [17, 83] Central Processing Unit (CPU), as listed in Table 17, with only a single example listing Advanced Micro Devices (AMD) [2]. There are also requirements for a large amount of Random Access Memory (RAM) in Table 17, with Xiao et al. [55] using 32 GB of Double Data Rate 4 (DDR4) Synchronous Dynamic Random-Access Memory (SDRAM), and as many as 80 CPUs on Linux and 504 GB of RAM used for ML by Spadon et al. [102]. In contrast, Zhao et al. [65] have modest requirements, with a 2.7 GHz CPU and 4 GB of RAM.

Table 18 is dedicated to the software specifications listed in various papers. Chondrodima et al. [17] are the only ones that use the NVIDIA Compute Unified Device Architecture (CUDA) Deep neural network (NN) library to directly and efficiently control GPU operations. Chondrodima et al. [17] also provide GitHub repository access, and Shin et al. [101] follow proper reproducibility practices as well. The e**X**treme **G**radient **Boost**ing (XGBoost) model developed by Petrovic et al. [57] uses Gini impurity to rank factors, such as SOG, by their influence, and this helps researchers outside the AI specialization understand the process. The integration of **SH**apley **A**dditive ex**P**lanations (SHAP) ensures the trust of human maritime experts, helping to pinpoint how much each part of the data contributed to a single prediction rather than just providing a random guess. The most commonly

Table 16 The GPU for selected papers reporting exact values

Citation	GPU
Ding et al. [73]	GTX 1650 GPU
Zhang et al. [18]	GTX 1080 Ti
Donandt et al. [72]	Two GPUs
Liang et al. [61]	RTX 2060
Sørensen et al. [71]	Tesla V100 SXM2 32 GB
Zhao et al. [63]	GTX 1650
Cao et al. [84]	GTX 3090 Ti 16 GB
Chondrodima et al. [17]	RTX 2080 Ti 11 GB
Gao et al. [89]	GTX 3050 Ti
Jurkus et al. [22]	RTX 3080 Vilnius University HPC
Li et al. [83]	RTX 1080 Ti 32 GB
Spadon et al. [93]	RTX A100 40 GB (Ampere) for DL
Wang and Xiao [90]	GTX 750 Ti
Zhang et al. [86]	RTX 3090 Ti
Zhao et al. [91]	GTX 1650
Zhao and Zhang [81]	RTX 3090 GPU
Drapier et al. [106]	RTX 4090
Jiang et al. [15]	RTX 2080 Ti
	GPU server (80 GB)
Jiang et al. [14]	RTX 2080 Ti
Li et al. [100]	GTX 1080 Ti
Nguyen and Fablet [108]	GTX 1080 Ti
Shin et al. [101]	GTX 3090 24 GB
Spadon et al. [102]	A100 40 GB
Xiao et al. [96]	RTX 3080 12 GB
Xue et al. [9]	RTX 3060 12 GB
Zhou et al. [99]	RTX 2080 Ti
Liu et al. [2]	RTX 3060

Table 17 The CPU and RAM for selected papers reporting exact values

Citation	CPU	RAM
Murray and Perera [70]	2.30 GHz	16 GB
Zhang et al. [77]	i5	8 GB
Liu et al. [66]	i7-7700K Quad Core	16 GB DDR4
Zhang et al. [18]	Not reported	24 GB
Liang et al. [61]	i7-9750 H 2.6 GHz	16 GB
Zhao et al. [65]	2.7 GHz	4 GB
Zhao et al. [63]	Not reported	16 GB
Cao et al. [84]	i7-7700 3.60 GHz	Not reported
Chondrodima et al. [17]	i9-9900KX	64 GB
Li et al. [83]	i9-11900U 3.60 GHz	Not reported
Mehri et al. [21]	i5 3.4 GHz	8 GB
Spadon et al. [93]	80 CPUs Linux for ML	504 GB for ML
	48 CPUs Linux for DL	126 GB for DL
Wang and Xiao [90]	Lenovo i5-1135G7 2.40 GHz	16 GB
Xiao et al. [55]	E5-2618LV3	32 GB DDR4
Jiang et al. [14]	Xeon E-2224 G	32 GB
Li et al. [100]	i7-11700F	Not reported
Li et al. [107]	M1 CPU	Not reported
Spadon et al. [102]	42 CPUs	128 GB
Xiao et al. [96]	i7-11700k	32 GB
Xue et al. [9]	Not reported	64 GB
Drapier et al. [106]	i9-13900K	24 GB
Liu et al. [2]	AMD Ryzen 7 5800 H	16 GB

used libraries are scikit-learn, Keras, and TensorFlow, which provide powerful ML and DL baselines, while lightweight alternatives include the Light Gradient Boosting Machine (LightGBM) and HMMs [80].

Most papers use Python within an environment, such as Spyder [22] or PyCharm [97], whereas others [3, 65] use MATLAB, a powerful alternative for signal processing. The primary Operating System (OS) is Windows, with examples for macOS [107] and Linux distributions [55, 86, 99], such as Ubuntu [96, 102] and Manjaro [106]. There are Python libraries dedicated to spatially aware coding, such as MovingPandas [21, 68, 76] and pyproj.Geod [22], as well as AISdb [102] for maritime experts.

4.3 Interpretability

The field of maritime trajectory prediction is shifting away from "black box" algorithms toward systems that explain their reasoning. Recent breakthroughs, as shown in Table 19, are making these models more transparent by employing specialized attention mechanisms and clear metrics to highlight the most important data points.

For example, Zhou et al. [3] use the Frequency-Enhanced Channel Attention Mechanism (FECAM) and the Discrete Cosine Transform (DCT) to demonstrate that the generated heatmaps align with real-world sea conditions and wave patterns, building trust in autonomous shipping by showing exactly how environmental factors influence decision-making.

Zhou et al. [99] introduced a dual-attention framework designed to handle the messy, non-linear nature of MMSI data. This system uses Trajectory Point Correlation (TPC) to spotlight critical movements, such as sharp turns, rather than relying solely on the most recent data. The second innovation introduced, Temporal Pattern Attention (TPA), helps the model recognize specific movement trends, including speed changes, ensuring important context over long voyages is never lost.

In the challenging conditions of the polar regions, Liu et al. [2] combined LSTM and KAN into a single approach. While standard Multi-layer Perceptron (MLP) models are

Table 18 The software requirement for selected papers reporting exact values

Citation	Software
Ding et al. [73]	Windows 10, Python: PyTorch 1.4.0
Wang et al. [19]	Python: Keras
You et al. [10]	Python: Keras
Liu et al. [66]	Python: PyTorch 1.6.0
Lu et al. [74]	Windows 10, Python 3.6.7: Numpy; PyTorch
Mehri et al. [76]	Python: MovingPandas
Zhang et al. [18]	Python 3.7.6: Keras 2.1.4; TensorFlow 1.14
Zhu [67]	Windows, Python: PyTorch
Anne et al. [68]	Python: MovingPandas
Liang et al. [61]	Windows 10 64-bit, Python: PyTorch 1.0
Yang et al. [69]	Python: Keras
Zhang et al. [16]	Python: TensorFlow
Zhao et al. [65]	Windows 10, Matlab 2019
Zhao et al. [63]	Python: PyTorch 1.10.1
Zheng et al. [79]	Python: TensorFlow
Cao et al. [84]	Python: Keras
Chondrodima et al. [17]	NVIDIA CUDA Deep NN library
	(https://github.com/DataStories-UniPi/VLF_VRF)
Jurkus et al. [22]	Windows 10, Spyder 4.1.5, Python 3.7.9: pyproj.Geod
	Keras; NumPy; TensorFlow
Li et al. [83]	Windows 10 64-bit, Python 3.9: PyTorch
Mehri et al. [21]	Python: MovingPandas
Petrovic et al. [57]	Python: Keras; SHAP; XGBoost
Spadon et al. [93]	Linux, Python: lightning; polylearn; scikit-extra; scikit-learn
	scikit-multiflow; CatBoost; LGBM; PyTorch; XGBoost
Wang and Xiao [90]	Windows 10, Python 3.8: PyTorch 1.10
Xiao et al. [55]	Ubuntu 16.04, Python 3.6.1: Keras 2.1.6
Zhang et al. [86]	Ubuntu, Python 3.6.9: PyTorch
Zhang et al. [80]	Python: hmmlearn
Zhao et al. [91]	Windows 10, Python: PyTorch
Zhao and Zhang [81]	Python: PyTorch
Bi et al. [98]	Python 3.7: Keras 2.1.4; PyTorch 4.0
Dong et al. [97]	Windows 10, PyCharm 2021, Python 3.7: Keras 3.1.1
Jiang et al. [14]	Windows 10, Python: scikit-learn; statsmodels
Jiang et al. [15]	NumPy; PyTorch 1.12.0; TensorFlow 2.7.0
Li et al. [100]	Windows 10, Python 3.8: PyTorch 2.0
Li et al. [107]	macOS, Python 3.10: PyTorch 2.4
Li et al. [8]	Python 3.9
Shin et al. [101]	Python: PyTorch (https://github.com/yuyolshin/AIS-ACNet)
Spadon et al. [102]	Ubuntu 20.04 LTS, Python: AISdb
Xiao et al. [96]	Ubuntu 20.0, Python 3.8: Tensorflow 2.15
Zhou et al. [99]	Ubuntu 20.04, Python: PyTorch
Drapier et al. [106]	Manjaro 23.1.3, Python: HuggingFace; PyTorch
Liu et al. [2]	Windows 11, Python 3.8
Wang et al. [105]	Python: PyTorch
Zhou et al. [3]	Matlab R2024a, Python: scikit-learn

Table 19 The selected papers using interpretability methods

Citation	Interpretability
Zhang et al. [18]	Attention visualization
Liu et al. [13]	Self-attention and multigraph representation
Petrovic et al. [57]	SHAP and Gini impurity
Xiao et al. [55]	Attention visualization
Bi et al. [98]	MHA visualization
Dong et al. [97]	CNN-MTABiGRU attention visualization
Nguyen and Fablet [108]	Attention weights visualization
Zhou et al. [99]	TPC and TPA
Liu et al. [2]	KAN
Zhou et al. [3]	Attention (FECAM and self-attention weights)

not transparent, with the logic obscured in fixed weights and activation layers, KAN architectures use adjustable mathematical functions directly on the network's connections and break down the complicated relationship between sea ice and ship movement into readable mathematical splines, and the reasoning is shown through clear transformations.

4.4 Quantitative comparisons of the surveyed methods using cross-study metrics

To competitively demonstrate the performance of all evaluated methods and prove the benefit of complex architectures despite the high computational demands, Table 20 reports the ADE and FDE as listed in the original works, as these are some of the most widely used trajectory prediction evaluation metrics, even outside the maritime domain, such as for pedestrians, aircraft, or land vehicles. As many papers evaluate a variable forecasting window, these values are also specified.

Gao et al. [62] report ADE and FDE at 30 s, with 0.0000092621° and 0.000019520°, respectively. Donandt et al. [72] use a longer minimum time frame of 150 s (11.71 m

ADE), extending to a maximum of 15 min (120.61 m FDE). Liu et al. [13] state that forecasting 10 steps (100 s) in advance results in ADE and FDE values of 63.769 m and 81.230 m, respectively, rising to 225.43 m and 270.33 m at 30 steps (300 s). Sørensen et al. [71] use a time horizon of 25 min to achieve a minimum FDE of 1.75 km, extending to 75 min at the cost of a much higher FDE at 5.07 km.

Han et al. [104] use short-term forecasts (6 min), so they report much lower ADE and FDE values, at 94.79 m and 157.82 m, respectively. Jiang et al. [14] prove that location matters, as they use 10 frames for both ZSI (ADE 13.825 m and FDE 24.515 m) and YSW (ADE 3.312 m and FDE 5.949 m) sites, while achieving radically different outcomes. Li et al. [107] achieve an ADE of 0.009° at 20 min, 40 min, and 60 min, while the FDE is minimal at 40 min (0.009°), and equal to 0.010° at 20 min and 60 min. Li et al. [8] use a time frame ranging from 5 min (ADE 0.0094° and FDE 0.0135°) to 60 min (ADE 0.0301° and FDE 0.0371°). Nguyen and Fablet [108] report FDE at 1 h (0.48 nmi) and 3 h (1.64 nmi), indicating a stark contrast over this timespan. Shin et al. [101] process AIS data using Auxiliary tasks and Convolutional Encoders Network (AIS-ACNet) [101], reporting ADE (0.107 square nmi) and FDE (0.320 nmi) at 15 min, which is much lower, as expected for short-term forecasting.

Xiao et al. [96] show the difference between results at N = 10 (5 min, FDE 0.215 km) and N = 30 (15 min, FDE 0.423 km). Zhang et al. [95] predict 5 points into the future (150 min), and the total ADE is 0.155°, latitude ADE is 0.0603°, longitude ADE is 0.0684°, COG ADE is 0.1227°, and SOG ADE is 0.0874 knots. Liu et al. [2] report values at 1 s, where the minimal ADE is 0.00456° for dataset a, and Dataset b at 30 s shows the highest ADE of 0.0468°. Wang et al. [105] show that ADE ranges from 0.7015 km (1 h) to 3.8271 km (6 h), proving that time constraints are of prime importance. Zhou et al. [3] deal with short-term forecasts, and at 1 min, the ADE is 0.0082 nmi, and the FDE is 0.0010 nmi, while at 10 min the ADE and FDE are 0.0578 nmi and 0.0157 nmi, respectively.

As some papers do not report ADE and FDE, we supplement the evaluation with RMSE for different prediction times in Table 21. However, there is a risk the reader must be aware of, as the data could be misleading if only looking at the table, and they may mistakenly think that one model's RMSE is better than another, but in reality, the sea areas, such as inland or offshore, and larger or smaller time windows tested by the two, are completely different.

In Table 21, CNN-LSTM-SE RMSE is between 0.0012° for 10 s and 0.0029° for 1 min, proving the influence of forecasting horizons [90]. Bidirectional Data-Driven Trajectory (BDD-T) prediction also shows a change in RMSE from 4 min (0.008°) to 2 h (0.041°) [55]. The bidirectional LSTM model from 2023 achieves low RMSE values (0.000355°) for a single future step, increasing to 0.000676° over five steps

Table 20 The reported ADE or FDE for different prediction horizons, datasets, or variables (results from different datasets and prediction durations are not directly comparable)

Citation	Description	ADE	FDE
Gao et al. [62]	30 s	0.0000092621°	0.000019520°
Donandt et al. [72]	150 s	11.71 m	–
	15 min	–	120.61 m
Liu et al. [13]	10 steps (100 s)	63.769 m	81.230 m
	20 steps (200 s)	142.57 m	178.04 m
	30 steps (300 s)	225.43 m	270.33 m
Sørensen et al. [71]	25 min	–	1.75 km
	50 min	–	2.53 km
	75 min	–	5.07 km
Han et al. [104]	6 min	94.79 m	157.82 m
Jiang et al. [14]	10 frames ZSI	13.825 m	24.515 m
	10 frames YSW	3.312 m	5.949 m
	10 frames YRW	5.599 m	9.989 m
Li et al. [107]	20 min	0.009°	0.010°
	40 min	0.009°	0.009°
	60 min	0.009°	0.010°
Li et al. [8]	5 min	0.0094°	0.0135°
	20 min	0.0136°	0.0197°
	40 min	0.0238°	0.0264°
	60 min	0.0301°	0.0371°
Nguyen and Fablet [108]	1 h	–	0.48 nmi
	2 h	–	0.94 nmi
	3 h	–	1.64 nmi
Shin et al. [101]	15 min	0.107 square nmi	0.320 nmi
Xiao et al. [96]	N = 10 (5 min)	–	0.215 km
	N = 20 (10 min)	–	0.331 km
	N = 30 (15 min)	–	0.423 km
Zhang et al. [95]	5 points (150 min)	0.155° (Total)	–
		0.0603° (Latitude)	–
		0.0684° (Longitude)	–
		0.1227° (COG)	–
		0.0874 knots (SOG)	–
Liu et al. [2]	1 s (Dataset a)	0.00456°	–
	10 s (Dataset a)	0.00527°	–
	30 s (Dataset a)	0.00682°	–
	1 s (Dataset b)	0.00488°	–

Table 20 continued

Citation	Description	ADE	FDE
	10 s (Dataset b)	0.00523°	–
	30 s (Dataset b)	0.0468°	–
	1 s (Dataset c)	0.00871°	–
	10 s (Dataset c)	0.0114°	–
	30 s (Dataset c)	0.0129°	–
Wang et al. [105]	1 h	0.7015 km	–
	2 h	1.1554 km	–
	3 h	1.7242 km	–
	6 h	3.8271 km	–
Zhou et al. [3]	1 min	0.0082 nmi	0.0010 nmi
	5 min	0.0325 nmi	0.0038 nmi
	10 min	0.0578 nmi	0.0157 nmi

[a]Metrics reported on heterogeneous datasets with different prediction horizon and geographic conditions; absolute values not directly comparable across rows

[86]. The Wavelet Transform (WT), Temporal Convolutional Networks (TCN), and Gated Recurrent Unit (GRU) (WTG) model follows a similar RMSE trend when shifting from 20 (0.050°) to 60 min (0.075°) [107]. VesNet provides forecasts ranging from 5 min (RMSE 0.0072°) to 120 min (RMSE 0.0682°) into the future, corresponding to previously listed expectations [15]. Finally, G-Trans RMSE is 0.009151° at 0.6 h and 0.036718° at 1.8 h, but the data do not match those of the other cited approaches [9].

The papers that specify other testing and training scenario characteristics beyond the forecasting horizon, along with their corresponding RMSEs, are listed in Table 22.

The Spatio-temporal feature-optimized Sequence-to-Sequence (ST-Seq2Seq) model achieved RMSE values of 0.00386° in Wuhan and 0.00849° in Chongqing [10]. A Multi-scale Convolutional Neural Network (MSCNN) with a Gated Recurrent Unit Attention Mechanism (GRU-AM), and an AutoRegressive (AR) model reaches RMSE values between 0.0001013° and 0.007917°, depending on the line and the direction [18]. The bidirectional LSTM [69] prediction RMSE varies from 139 m for vessel 2 to 211.79 m for vessel 9. The k-GCN-LSTM RMSE was smallest in case C (0.016°) and largest in case B (0.0637°), indicating that

Table 21 The RMSE for selected trajectory prediction papers and models, with the prediction horizon specified as time in seconds, minutes, or hours, or number of points in the past (input) and future (output) for the testing scenario, where applicable

Citation	Model	Horizon	RMSE
Wang and Xiao [90]	CNN-LSTM-SE	Ship-1, 10 s	0.0014°
		Ship-1, 30 s	0.0022°
		Ship-1, 1 min	0.0029°
		Ship-2, 10 s	0.0012°
		Ship-2, 30 s	0.0024°
		Ship-2, 1 min	0.0025°
Xiao et al. [55]	BDD-T	4 min	0.008°
		8 min	0.016°
		20 min	0.025°
		30 min	0.033°
		1 h	0.031°
		2 h	0.041°
Zhang et al. [86]	BiLSTM LSTM	10 → 1	0.000355°
		10 → 2	0.000359°
		10 → 3	0.000385°
		10 → 4	0.000426°
		10 → 5	0.00048°
		First point	0.000355°
		Second point	0.00037°
		Third point	0.000437°
		Fourth point	0.00054°
		Fifth point	0.000676°
Li et al. [107]	WTG	20 min	0.050°
		40 min	0.067°
		60 min	0.075°
Jiang et al. [15]	VesNet	5 min	0.0072°
		10 min	0.0097°
		30 min	0.0151°
		60 min	0.029°
		120 min	0.0682°
Xue et al. [9]	G-Trans	0.6 h	0.009151°
		1.2 h	0.031367°
		1.8 h	0.036718°

[a]Metrics reported on heterogeneous datasets with different prediction horizons and geographic conditions; absolute values not directly comparable across rows

Table 22 The RMSE for selected trajectory prediction papers and models, with the explanation for the testing scenario where applicable

Citation	Model	Scenario	RMSE
You et al. [10]	ST-Seq2Seq	Wuhan	0.00386°
		Chongqing	0.00849°
Zhang et al. [18]	MSCNN Fusion GRU-AM	AR	0.002728°
		Line 1, Forward	0.000635°
		Line 1, Reverse	0.00086°
		Line 1, Final	0.000401°
		Line 2, Forward	0.003054°
		Line 2, Reverse	0.007917°
		Line 2, Final	0.002614°
		Line 3, Forward	0.000648°
		Line 3, Reverse	0.0001013°
		Line 3, Final	0.000521°
Yang et al. [69]	Bi-LSTM	Average	169.17 m
		Vessel 1	157 m
		Vessel 2	139 m
		Vessel 3	194 m
		Vessel 4	156 m
		Vessel 5	174 m
		Vessel 6	195 m
		Vessel 7	170.53 m
		Vessel 8	183.5 m
		Vessel 9	211.79 m
		Vessel 10	206.81 m
Zhao et al. [63]	k-GCN-LSTM	Case A	0.0326°
		Case B	0.0637°
		Case C	0.016°
Petrovic et al. [57]	LSTM-BPSO	Average	0.009985°
Xiao et al. [55]	BDD-T	Average	0.025°
Zhang et al. [86]	BiLSTM LSTM	Ablation	0.000479°
Bi et al. [98]	CNNGRU-MHA	CNNGRU-MHA	0.0127°
Zhang et al. [95]	S2S-MSA	Ablation	0.271°

[a]Metrics reported on heterogeneous datasets with different prediction horizons and geographic conditions; absolute values not directly comparable across rows

performance varies [63]. The average RMSE of the Long Short-Term Memory Boosted Particle Swarm Optimization (LSTM-BPSO) is 0.009985° [57]. The BDD-T [55] prediction model has an average RMSE of 0.025°, which is much higher, but the dataset is not similar to others. The bidirectional LSTM [86] RMSE value is 0.000479° in ablation, and the RMSE of the Sequence-to-Sequence Based Multi-semantic Network with Attention (S2S-MSA) is 0.271° in the ablation study [95], but this paper again varies the input.

CNN and GRU based on MHA (CNNGRU-MHA) RMSE is 0.0127° [98], which is between the two previously cited values for other models in ablation [86, 95].

The papers that separately evaluate RMSE for longitude and latitude are shown in Table 23. An RNN outperforms simple backpropagation, with RMSE values for longitude and latitude of 0.00000778° and 0.0000131°, respectively, compared to 0.0000713° and 0.00322°, respectively [67]. The Attribute Correlation Attention (ACoAtt) LSTM RMSE ranges from the straight-line scenario (lowest values of 0.000356° and 0.000061° for longitude and latitude, respectively) to the maximum error at the largest trajectory length of 20 points (0.00293° and 0.00122° for longitude and latitude, respectively) [100]. For CNNGRU-MHA, longitude and latitude RMSE are 0.0139° and 0.0115°, respectively [98]. CNNGRU-MHA values [98] are much lower than the ablation study of S2S-MSA [95], with RMSE equal to 0.1019° and 0.0952° for longitude and latitude, respectively. It is also worth noting that the largest longitude and latitude were observed for D-TCN, with 0.208° (longitude in case 1) and 0.201° (latitude in case 2), although their testing conditions differed significantly from those of other approaches [16]. As expected, LSTM RMSE increases as the time horizon extends further into the future, with 0.002705° and 0.001687° for longitude and latitude RMSE at step 1 (2 min), and 0.014852° and 0.055091° for longitude and latitude RMSE at step 20 (40 min) [99].

The papers that also demonstrate RMSE for SOG and COG are contained in Table 24. Similar findings to those for longitude and latitude are observed for SOG and COG RMSE, with values at step 1 (2 min) of 0.097449 knots and 1.277275°, respectively, rising to 0.674251 knots and 5.954145° at step 20 (40 min) [99].

S2S-MSA ablation [95] showed that SOG RMSE was 0.1249 knots, between the previously cited minimum and maximum, while COG RMSE was much lower at 0.1725°. However, the high variability in the training and testing data between these studies must be considered [95, 99].

Table 23 The longitude and latitude RMSE for selected trajectory prediction papers and models, with the explanation for the testing scenario where applicable (results from different datasets and prediction durations are not directly comparable)

Citation	Model	Scenario	Lon. RMSE	Lat. RMSE
Zhu [67]	Backpropagation	Backpropagation	0.0000713°	0.00322°
	RNN	RNN	0.00000778°	0.0000131°
Zhang et al. [16]	D-TCN	Case 1	0.208°	0.165°
		Case 2	0.105°	0.201°
Bi et al. [98]	CNNGRU-MHA	CNNGRU-MHA	0.0139°	0.0115°
Li et al. [100]	ACoAtt–LSTM	Straight-line	0.000356°	0.000061°
		Curved maneuver	0.000437°	0.000411°
		Length 5	0.00088°	0.00063°
		Length 10	0.00149°	0.00084°
		Length 20	0.00293°	0.00122°
		Straight (verified)	0.000612°	0.000554°
		Curved (verified)	0.001057°	0.00127°
Zhang et al. [95]	S2S-MSA	Ablation	0.1019°	0.0952°
Zhou et al. [99]	LSTM	Step 1 (2 min)	0.002705°	0.001687°
		Step 5 (10 min)	0.005393°	0.006556°
		Step 10 (20 min)	0.007103°	0.019978°
		Step 15 (30 min)	0.008991°	0.036784°
		Step 20 (40 min)	0.014852°	0.055091°

[a]Metrics reported on heterogeneous datasets with different prediction horizons and geographic conditions; absolute values not directly comparable across rows

Table 24 The SOG and COG RMSE for selected trajectory prediction papers and models, with the explanation for the testing scenario where applicable (results from different datasets and prediction durations are not directly comparable)

Citation	Model	Scenario	SOG RMSE	COG RMSE
Zhang et al. [95]	S2S-MSA	Ablation	0.1249 knots	0.1725°
Zhou et al. [99]	LSTM	Step 1 (2 min)	0.097449 knots	1.277275°
Zhou et al. [99]	LSTM	Step 5 (10 min)	0.101414 knots	2.34561°
Zhou et al. [99]	LSTM	Step 10 (20 min)	0.241574 knots	3.541244°
Zhou et al. [99]	LSTM	Step 15 (30 min)	0.475864 knots	4.751432°
Zhou et al. [99]	LSTM	Step 20 (40 min)	0.674251 knots	5.954145°

[a]Metrics reported on heterogeneous datasets with different prediction horizons and geographic conditions; absolute values not directly comparable across rows

5 Conclusion

This survey reveals that vessel trajectory forecasting is rapidly evolving and shifting from rule-based and statistical models toward increasingly sophisticated ML and DL approaches. By covering literature up to 2025, this review highlights a decisive methodological shift toward advanced architectures that address long-standing limitations in scalability and adaptability. By evaluating diverse papers, we emphasize the emergence of Transformer-based and GNN models as the state-of-the-art for capturing long-range spatiotemporal dependencies and multi-vessel interactions, respectively. While classical methods, such as Bayesian inference, provide foundational transparency, their performance in dynamic, long-range prediction is increasingly surpassed by these modern, data-driven systems. Despite the limitations of such simplistic processing, the use of maximum likelihood estimation in stochastic process techniques for real-time applications has higher computational efficiency and lower processing load. Graph-based and clustering approaches offer structural insights into navigational patterns, but they require complementary dynamic models.

Despite the impressive performance of DL and Transformer-based models, their high computational complexity poses challenges for real-world deployment in resource-constrained environments, such as onboard maritime systems. Additionally, the reliability of AIS data remains a critical concern. Recent increases in spoofing and intentional AIS signal manipulation, often associated with illicit activities or geopolitical strategies, undermine data integrity, underscoring the urgent need for robust anomaly-detection mechanisms.

Recurrent models implemented as LSTM and GRU architectures offer strong baseline performance, particularly when augmented with attention mechanisms and contextual preprocessing. Attention-based and RNN architectures handle sharp turns and irregular trajectories better than probabilistic models.

The authors of this paper provided a benchmark of several RNN models [67], as well as Bayesian and Markov chain models [104], showing that even basic RNN and LSTM architectures, combined with thoughtful input representation, can match or outperform probabilistic models. The study showed that attention architectures and Transformers achieve the best real-world performance. The trends highlight hybrid systems that combine the strengths of various models. Future work should prioritize explainability by leveraging technologies such as attention-weight visualization to provide transparency into neural decision-making. Additionally, model compression techniques, including knowledge distillation and parameter pruning, are essential for deploying complex architectures on resource-constrained shipboard hardware. Enhancing cross-domain generalization via advanced transfer learning strategies will be critical for adapting models across diverse geographies and vessel types. Finally, standardizing benchmark datasets will remain vital to enhance global reproducibility in maritime forecasting.

Author contributions Lucija Žužić: Conceptualization, Methodology, Software, Validation, Investigation, Data Curation, Writing—Original Draft, Visualization.
Nikola Lopac: Conceptualization, Validation, Formal analysis, Investigation, Resources, Writing—Original Draft, Writing—Review & Editing, Supervision.
Marko Šimic: Conceptualization, Validation, Formal analysis, Investigation, Resources, Writing—Original Draft, Writing—Review & Editing, Supervision.
Jonatan Lerga: Conceptualization, Methodology, Validation, Formal analysis, Investigation, Resources, Writing—Original Draft, Writing—Review & Editing, Supervision, Project administration, Funding acquisition.
Lucija Žužić, Nikola Lopac, Marko Šimic, and Jonatang Lerga had the idea for the article, Lucija Žužić performed the literature search and data analysis, and Lucija Žužić, Nikola Lopac, Marko Šimic, and Jonatang Lerga drafted and/or critically revised the work.

Funding This work was fully supported by the IRI S3 ("Povećanje razvoja novih proizvoda i usluga koji proizlaze iz aktivnosti istraživanja i razvoja") project, Grant No. PK.1.1.12.0066; the EU Horizon project INNO2MARE Grant No. 101087348; the Ministry of Science, Education and Youth of the Republic of Croatia through the bilateral Croatian-Slovenian project "Predicting Anomalous Trajectories Using Machine Learning" and the European Union—NextGenerationEU project Grant No. uniri-mzi-25-1 implemented through the University of Rijeka.

Data Availability Data sharing is not applicable to this article as no new datasets were generated for this manuscript. All data from the papers aggregated in this review article are included in the published figures, tables, and bibliography.

Declarations

Conflict of interest The authors declare no conflict of interest.

References

1. Liu Z, Wang Y, Vaidya S, Ruehle F, Halverson J, Soljacic M, Hout TY, Tegmark M (2025) KAN: Kolmogorov–Arnold networks. In: The thirteenth international conference on learning representations, Singapore, vol 2025. OpenReview, Newton Highlands, MA, USA. pp 1–47. https://openreview.net/forum?id=Ozo7qJ5vZi. Accessed 17 Apr 2026
2. Liu W, Shen H, Hu Y, Hsieh TH, Wang S, Han B (2025) Polar ship trajectory prediction based on Kolmogorov–Arnold networks and LSTM. Ocean Eng 336:121702. https://doi.org/10.1016/j.oceaneng.2025.121702
3. Zhou X, Zheng F, Yang H, Guo N, Yu A, Wang J (2025) ST-FEiTNet: a trajectory prediction model for complex sea states via multiscale spatiotemporal feature extraction and cross-modal frequency enhancement. Ocean Eng 342:122922. https://doi.org/10.1016/j.oceaneng.2025.122922
4. Üney M, Millefiori LM, Braca P (2019) Data driven vessel trajectory forecasting using stochastic generative models. In: ICASSP 2019—2019 IEEE international conference on acoustics, speech and signal processing (ICASSP), Brighton, UK. IEEE, New York, NY, USA, pp 8459–8463. https://doi.org/10.1109/ICASSP.2019.8683444. Accessed 17 Apr 2026
5. Rong H, Teixeira AP, Soares CG (2019) Ship trajectory uncertainty prediction based on a Gaussian process model. Ocean Eng 182:499–511. https://doi.org/10.1016/j.oceaneng.2019.04.024
6. Suo Y, Chen W, Claramunt C, Yang S (2020) A ship trajectory prediction framework based on a recurrent neural network. Sensors 20(18):5133. https://doi.org/10.3390/s20185133
7. Gao D, Zhu Y, Yan K, Soares CG (2024) Deep learning-based framework for regional risk assessment in a multi-ship encounter situation based on the transformer network. Reliab Eng Syst Saf 241:109636. https://doi.org/10.1016/j.ress.2023.109636
8. Li Y, Wang J, Li T, Fu Z, (2024) TrAISformer: spatio-temporal ship trajectory prediction based on transformer. In: 2024 5th international seminar on artificial intelligence, networking and information technology (AINIT), Nanjing, China. IEEE New York NY USA, pp 1099–1104. https://doi.org/10.1109/AINIT61980.2024.10581516. Accessed 17 Apr 2026
9. Xue H, Wang S, Xia M, Guo S (2024) G-Trans: a hierarchical approach to vessel trajectory prediction with GRU-based transformer. Ocean Eng 300:117431. https://doi.org/10.1016/j.oceaneng.2024.117431
10. You L, Xiao S, Peng Q, Claramunt C, Han X, Guan Z, Zhang J (2020) ST-Seq2Seq: a spatio-temporal feature-optimized Seq2Seq model for short-term vessel trajectory prediction. IEEE Access 8:218565–218574. https://doi.org/10.1109/ACCESS.2020.3041762
11. Zhang C, Bin J, Liu Z (2024) TrajBERT-DSSM: deep bidirectional transformers for vessel trajectory understanding and destination prediction. Ocean Eng 297:117147. https://doi.org/10.1016/j.oceaneng.2024.117147
12. Hao S, Liu J, Zhang X, Shi Q, Zhi J, Jiang X (2023) Multi-ship trajectory prediction framework for high-density maritime traffic areas based on BI-GRU and GAT. In: 2023 11th international conference on information systems and computing technol-

ogy (ISCTech), Qingdao, China. IEEE, New York, NY, USA, pp 333–337. https://doi.org/10.1109/ISCTech60480.2023.00067. Accessed 17 Apr 2026

13. Liu RW, Liang M, Nie J, Yuan Y, Xiong Z, Yu H, Guizani N (2022) STMGCN: mobile edge computing-empowered vessel trajectory prediction using spatio-temporal multigraph convolutional network. IEEE Trans Ind Inform 18(11):7977–7987. https://doi.org/10.1109/TII.2022.3165886
14. Jiang J, Zuo Y, Xiao Y, Zhang W, Li T (2024) STMGF-Net: a spatiotemporal multi-graph fusion network for vessel trajectory forecasting in intelligent maritime navigation. IEEE Trans Intell Transp Syst 25(12):21367–21379. https://doi.org/10.1109/TITS.2024.3465234
15. Jiang F, Wang H, Li Y (2024) VesNet: a vessel network for jointly learning route pattern and future trajectory. ACM Trans Intell Syst Technol 15(2):34. https://doi.org/10.1145/3639370
16. Zhang K, Zhang C, Zhu Q, Gu Y, Liu C, (2022) Ship trajectory D-TCN prediction method based on satellite remote sensing positioning data. In: 2022 China automation congress (CAC), Xiamen, China. IEEE New York NY USA, pp 1419–1424. https://doi.org/10.1109/CAC57257.2022.10055335. Accessed 17 Apr 2026
17. Chondrodima E, Pelekis N, Pikrakis A, Theodoridis Y (2023) An efficient LSTM neural network-based framework for vessel location forecasting. IEEE Trans Intell Transp Syst 24(5):4872–4888. https://doi.org/10.1109/TITS.2023.3247993
18. Zhang L, Zhang J, Niu J, Wu QMJ, Li G (2021) Track prediction for HF radar vessels submerged in strong clutter based on MSCNN fusion with GRU-AM and AR model. Remote Sens 13(11):2164. https://doi.org/10.3390/rs13112164
19. Wang Y, Cheng H, Zhou X, Luo W, Zhang H (2020) Moving ship detection and movement prediction in remote sensing videos. Int Arch Photogramm Remote Sens Spat Inf Sci XLIII-B2-2020:1303–1308. https://doi.org/10.5194/isprs-archives-XLIII-B2-2020-1303-2020. Accessed 17 Apr 2026
20. Li W, Zhang C, Ma J, Jia C (2019) Long-term vessel motion predication by modeling trajectory patterns with AIS data. In: 2019 5th international conference on transportation information and safety (ICTIS), Liverpool, UK. IEEE, New York, NY, USA, pp 1389–1394. https://doi.org/10.1109/ICTIS.2019.8883596. Accessed 17 Apr 2026
21. Mehri S, Alesheikh AA, Basiri A (2023) A context-aware approach for vessels' trajectory prediction. Ocean Eng 282:114916. https://doi.org/10.1016/j.oceaneng.2023.114916
22. Jurkus R, Venskus J, Treigys P (2023) Application of coordinate systems for vessel trajectory prediction improvement using a recurrent neural networks. Eng Appl Artif Intell 123:106448. https://doi.org/10.1016/j.engappai.2023.106448
23. Ristic B, La Scala B, Morelande M, Gordon N (2008) Statistical analysis of motion patterns in AIS Data: Anomaly detection and motion prediction. In: 2008 11th international conference on information fusion, Cologne, Germany. IEEE, New York, NY, USA, pp 1–7. https://ieeexplore.ieee.org/document/4632190. Accessed 17 Apr 2026
24. Lane RO, Nevell DA, Hayward SD, Beaney TW (2010) Maritime anomaly detection and threat assessment. In: 2010 13th International conference on information fusion, Edinburgh, UK. IEEE, New York, NY, USA, pp 1–8. https://doi.org/10.1109/ICIF.2010.5711998. Accessed 17 Apr 2026
25. Katsilieris F, Braca P, Coraluppi S (2013) Detection of malicious AIS position spoofing by exploiting radar information. In: Proceedings of the 16th international conference on information fusion, Istanbul, Turkey. IEEE, New York, NY, USA, pp 1196–1203. https://ieeexplore.ieee.org/document/6641132. Accessed 17 Apr 2026
26. Prasad P, Vatsal V, Roy Chowdhury R (2021) Maritime vessel route extraction and automatic information system (AIS) spoofing detection. In: 2021 International conference on advances in electrical, computing, communication and sustainable technologies (ICAECT), Bhilai, India. IEEE, New York, NY, USA, pp 1–11. https://doi.org/10.1109/icaect49130.2021.9392536. Accessed 17 Apr 2026
27. Young DL (2019) Deep nets spotlight illegal, unreported, unregulated (IUU) fishing. In: 2019 IEEE applied imagery pattern recognition workshop (AIPR), Washington, DC, USA. IEEE New York NY USA, pp 1–7. https://doi.org/10.1109/AIPR47015.2019.9174577. Accessed 17 Apr 2026
28. d'Afflisio E, Braca P, Millefiori LM, Willett P (2018) Detecting anomalous deviations from standard maritime routes using the Ornstein–Uhlenbeck process. IEEE Trans Signal Process 66(24):6474–6487. https://doi.org/10.1109/TSP.2018.2875887
29. Milios A, Bereta K, Chatzikokolakis K, Zissis D, Matwin S (2019) Automatic fusion of satellite imagery and AIS data for vessel detection. In: 2019 22th international conference on information fusion (FUSION), Ottawa, ON, Canada. IEEE, New York, NY, USA, pp 1–5. https://doi.org/10.23919/FUSION43075.2019.9011339. Accessed 17 Apr 2026
30. Kowalska K, Peel L (2012) Maritime anomaly detection using Gaussian process active learning. In: 2012 15th international conference on information fusion, Singapore. IEEE, New York, NY, USA, pp 1164–1171. https://ieeexplore.ieee.org/document/6289940. Accessed 17 Apr 2026
31. Zhang M, Montewka J, Manderbacka T, Kujala P, Hirdaris S (2021) A big data analytics method for the evaluation of ship–ship collision risk reflecting hydrometeorological conditions. Reliab Eng Syst Saf 213:107674. https://doi.org/10.1016/j.ress.2021.107674
32. Shahir AY, Tayebi MA, Glässer U, Charalampous T, Zohrev, Z, Wehn H (2019) Mining vessel trajectories for illegal fishing detection. In: 2019 IEEE international conference on big data (big data), Los Angeles, CA, USA. IEEE, New York, NY, USA, pp 1917–1927. https://doi.org/10.1109/BigData47090.2019.9006545. Accessed 17 Apr 2026
33. Singh SK, Heymann F, (2020) Machine learning-assisted anomaly detection in maritime navigation using AIS data. In: 2020 IEEE/ION position, location and navigation symposium (PLANS), Portland, OR, USA. IEEE New York NY USA, pp 832–838. https://doi.org/10.1109/PLANS46316.2020.9109806. Accessed 17 Apr 2026
34. Mazzarella F, Vespe M, Alessandrini A, Tarchi D, Aulicino G, Vollero A (2017) A novel anomaly detection approach to identify intentional AIS on-off switching. Expert Syst Appl 78:110–123. https://doi.org/10.1016/j.eswa.2017.02.011
35. Mazzarella F, Vespe M, Tarchi D, Aulicino G, Vollero A (2016) AIS reception characterisation for AIS on/off anomaly detection. In: 2016 19th international conference on information fusion (FUSION), Heidelberg, Germany. IEEE, New York, NY, USA, pp 1867–1873. https://ieeexplore.ieee.org/document/7528110. Accessed 17 Apr 2026
36. Singh SK, Heymann F (2020) On the effectiveness of AI-assisted anomaly detection methods in maritime navigation. In: 2020 IEEE 23rd international conference on information fusion (FUSION), Rustenburg, South Africa. IEEE, New York, NY, USA, pp 1–7. https://doi.org/10.23919/fusion45008.2020.9190533. Accessed 17 Apr 2026
37. d'Afflisio E, Braca P, Chisci L, Battistelli G, Willett P (2021) Maritime anomaly detection of malicious data spoofing and stealth deviations from nominal route exploiting heterogeneous sources of information. In: 2021 IEEE 24th international conference on information fusion (FUSION), Sun City, South Africa. IEEE, New York, NY, USA, pp 1–7. https://doi.org/10.23919/fusion49465.2021.9627049. Accessed 17 Apr 2026

38. d'Afflisio E, Braca P, Willett P (2021) Malicious AIS spoofing and abnormal stealth deviations: a comprehensive statistical framework for maritime anomaly detection. IEEE Trans Aerosp Electron Syst 57(4):2093–2108. https://doi.org/10.1109/taes.2021.3083466
39. Ford J, Peel D, Kroodsma D, Hardesty B, Rosebrock U, Wilcox C (2018) Detecting suspicious activities at sea based on anomalies in automatic identification systems transmissions. PLoS ONE 13(8):e0201640. https://doi.org/10.1371/journal.pone.0201640
40. Javier T, Joaquim F, Guillermo F, Elisabet L, Ettore C, Silvia P, Ciro G (2025) IEC-61108-7 SBAS standard for shipborne receivers: preliminary testing validation activities. Eng Proc 88(1):48. https://doi.org/10.3390/engproc2025088048
41. Orbán J (2025) Overview of GNSS interference risks in transport safety and resilient responses. Eng Proc 113(1):42. https://doi.org/10.3390/engproc2025113042
42. Rizzi FG, Grundhöfer L, Gewies S, Hehenkamp N (2026) Enhancing maritime navigation: a novel approach to validate GNSS solutions with a single R-mode station. Eng Proc 126(1):19. https://doi.org/10.3390/engproc2026126019
43. Zheng H, Hu Q, Yang C, Mei Q, Wang P, Li K (2023) Identification of spoofing ships from automatic identification system data via trajectory segmentation and isolation forest. J Mar Sci Eng 11(8):1516. https://doi.org/10.3390/jmse11081516
44. Hauser JIM, Lesjak R, Ghafi HK (2026) GNSS interference along a highway near an aircraft approach lane: a 5-month study. Eng Proc 126(1):46. https://doi.org/10.3390/engproc2026126046
45. GPSPATRON (2025) Maritime GNSS interference worldwide: a cumulative analysis 2025 | GPSPATRON.com—gpspatron.com. https://gpspatron.com/maritime-gnss-interference-worldwide-a-cumulative-analysis-2025. Accessed 17 Apr 2026
46. MarineTraffic (2026) MarineTraffic: global ship tracking intelligence | AIS Marine Traffic—marinetraffic.com. https://www.marinetraffic.com. Accessed 17 Apr 2026
47. AISHub (2025) AIS Dispatcher—free AIS data sharing tool | AISHub—aishub.net. https://www.aishub.net/ais-dispatcher. Accessed 17 Apr 2026
48. Kress M, Mitchell K (2023) AIS data: an overview of free sources. Engineer Research and Development Center. US Army Corps of Engineers. https://doi.org/10.21079/11681/46491. Accessed 17 Apr 2026
49. USCG (2025) AIS historical request form | Navigation Center—navcen.uscg.gov. https://www.navcen.uscg.gov/contact/ais-historical-request. Accessed 17 Apr 2026
50. MarineCadastre (2025) MarineCadastre.gov | Vessel Traffic Data—marinecadastre.gov. https://marinecadastre.gov/ais. Accessed 17 Apr 2026
51. SeaVision (2026) SeaVision—seavision.volpe.dot.gov. https://seavision.volpe.dot.gov. Accessed 17 Apr 2026
52. MSSI (2026) MSSIS: Home—mssis.volpe.dot.gov. https://mssis.volpe.dot.gov. Accessed 17 Apr 2026
53. GlobalMaritimeTraffic (2026) Global maritime traffic | Ship AIS Navigation Data & Maps—globalmaritimetraffic.org. https://globalmaritimetraffic.org. Accessed 17 Apr 2026
54. ArcGIS (2026) vessel-traffic—livingatlas.arcgis.com. https://livingatlas.arcgis.com/vessel-traffic. Accessed 17 Apr 2026
55. Xiao Y, Li X, Yao W, Chen J, Hu Y (2023) Bidirectional data-driven trajectory prediction for intelligent maritime traffic. IEEE Trans Intell Transp Syst 24(2):1773–1785. https://doi.org/10.1109/TITS.2022.3219998
56. Ray C, Dréo R, Camossi E, Jousselme AL, Iphar C (2019) Heterogeneous integrated dataset for maritime intelligence, surveillance, and reconnaissance. Data Brief 25:104141. https://doi.org/10.1016/j.dib.2019.104141
57. Petrovic A, Damaševičius R, Jovanovic L, Toskovic A, Simic V, Bacanin N, Zivkovic M, Spalević P (2023) Marine vessel classification and multivariate trajectories forecasting using metaheuristics-optimized eXtreme gradient boosting and recurrent neural networks. Appl Sci 13(16):9181. https://doi.org/10.3390/app13169181
58. Erdönmez ES (2022) AIS Dataset—kaggle.com. https://www.kaggle.com/datasets/eminserkanerdonmez/ais-dataset. Accessed 17 Apr 2026
59. Gulisano V, Jerzak Z, Smirnov P, Strohbach M, Ziekow H, Zissis D (2018) The DEBS 2018 grand challenge. In: DEBS '18: proceedings of the 12th ACM international conference on distributed and event-based systems, Hamilton, NZ. ACM, New York, NY, USA, pp 191–194. https://doi.org/10.1145/3210284.3220510. Accessed 17 Apr 2026
60. Karataş GB, Karagoz P, Ayran O (2020) Trajectory prediction for maritime vessels using AIS data. In: MEDES '20: proceedings of the 12th international conference on management of digital EcoSystems, UAE. ACM, New York, NY, USA, pp 48–54. https://doi.org/10.1145/3415958.3433079. Accessed 17 Apr 2026
61. Liang M, Liu RW, Zhan Y, Li H, Zhu F, Wang FY (2022) Fine-grained vessel traffic flow prediction with a spatio-temporal multigraph convolutional network. IEEE Trans Intell Transp Syst 23(12):23694–23707. https://doi.org/10.1109/TITS.2022.3199160
62. Gao DW, Zhu YS, Zhang JF, He YK, Yan K, Yan BR (2021) A novel MP-LSTM method for ship trajectory prediction based on AIS data. Ocean Eng 228:108956. https://doi.org/10.1016/j.oceaneng.2021.108956
63. Zhao J, Yan Z, Chen X, Han B, Wu S, Ke R (2022) k-GCN-LSTM: a k-hop graph convolutional network and long-short-term memory for ship speed prediction. XXPhys A 606:128107. https://doi.org/10.1016/j.physa.2022.128107
64. Pan N, Ding Y, Fu J, Wang J, Zheng H (2021) Research on ship arrival law based on route matching and deep learning. J Phys: Conf Ser 1952(2):022023. https://doi.org/10.1088/1742-6596/1952/2/022023
65. Zhao J, Lu J, Chen X, Yan Z, Yan Y, Sun Y (2022) High-fidelity data supported ship trajectory prediction via an ensemble machine learning framework. XXPhys A 586:126470. https://doi.org/10.1016/j.physa.2021.126470
66. Liu RW, Liang M, Nie J, Deng X, Xiong Z, Kang J, Yang H, Zhang Y (2021) Intelligent data-driven vessel trajectory prediction in marine transportation cyber-physical system. In: 2021 IEEE international conferences on internet of things (iThings) and IEEE green computing & communications (GreenCom) and IEEE cyber, physical & social computing (CPSCom) and IEEE smart data (SmartData) and IEEE congress on cybermatics (Cybermatics), Melbourne, Australia. IEEE New York NY USA, pp 314–321. https://doi.org/10.1109/iThings-GreenCom-CPSCom-SmartData-Cybermatics53846.2021.00058. Accessed 17 Apr 2026
67. Zhu F (2021) Ship short-term trajectory prediction based on RNN. J Phys: Conf Ser 2025(1):012023. https://doi.org/10.1088/1742-6596/2025/1/012023
68. Anne D, Suhardi S, Muhamad W (2022) Prediction of ship track anomaly based on AIS data using long short-term memory (LSTM) and DBSCAN. In: 2022 International conference on information technology systems and innovation (ICITSI), Bandung, Indonesia. IEEE, New York, NY, USA, pp 107–112. https://doi.org/10.1109/ICITSI56531.2022.9970940. Accessed 17 Apr 2026
69. Yang CH, Wu CH, Shao JC, Wang YC, Hsieh CM (2022) AIS-based intelligent vessel trajectory prediction using Bi-LSTM. IEEE Access 10:24302–24315. https://doi.org/10.1109/ACCESS.2022.3154812
70. Murray B, Perera LP (2020) A dual linear autoencoder approach for vessel trajectory prediction using historical AIS

data. Ocean Eng 209:107478. https://doi.org/10.1016/j.oceaneng.2020.107478
71. Sørensen KA, Heiselberg P, Heiselberg H (2022) Probabilistic maritime trajectory prediction in complex scenarios using deep learning. Sensors 22(5):2058. https://doi.org/10.3390/s22052058
72. Donandt K, Böttger K, Söffker D (2022) Short-term inland vessel trajectory prediction with encoder-decoder models. In: 2022 IEEE 25th international conference on intelligent transportation systems (ITSC), Macau, China. IEEE, New York, NY, USA, pp 974–979. https://doi.org/10.1109/ITSC55140.2022.9922148. Accessed 17 Apr 2026
73. Ding M, Su W, Liu Y, Zhang J, Li J, Wu J (2020) A novel approach on vessel trajectory prediction based on variational LSTM. In: 2020 IEEE international conference on artificial intelligence and computer applications (ICAICA), Dalian, China. IEEE, New York, NY, USA, pp 206–211. https://doi.org/10.1109/ICAICA50127.2020.9182537. Accessed 17 Apr 2026
74. Lu B, Lin R, Zou H (2021) A novel CNN-LSTM Method for ship trajectory prediction. In: 2021 IEEE 23rd international conference on high performance computing & communications; 7th international conference on data science & systems; 19th international conference on smart city; 7th international conference on dependability in sensor, cloud & big data systems & application (HPCC/DSS/SmartCity/DependSys), Haikou, Hainan, China. IEEE New York NY USA, pp 2431–2436. https://doi.org/10.1109/HPCC-DSS-SmartCity-DependSys53884.2021.00366. Accessed 17 Apr 2026
75. Zhang S, Wang L, Zhu M, Chen S, Zhang H, Zeng Z (2021) A bi-directional LSTM ship trajectory prediction method based on attention mechanism. In: 2021 IEEE 5th advanced information technology, electronic and automation control conference (IAEAC), Chongqing, China. IEEE New York NY USA, pp 1987–1993. https://doi.org/10.1109/IAEAC50856.2021.9391059. Accessed 17 Apr 2026
76. Mehri S, Alesheikh AA, Basiri A (2021) A contextual hybrid model for vessel movement prediction. IEEE Access 9:45600–45613. https://doi.org/10.1109/ACCESS.2021.3066463
77. Zhang Z, Ni G, Xu Y (2020) Ship trajectory prediction based on LSTM neural network. In: 2020 IEEE 5th information technology and mechatronics engineering conference (ITOEC), Chongqing, China. IEEE New York NY USA, pp 1356–1364. https://doi.org/10.1109/ITOEC49072.2020.9141702. Accessed 17 Apr 2026
78. NOAA (2026) NOAA Office for Coastal Management—coast.noaa.gov. https://coast.noaa.gov. Accessed 17 Apr 2026
79. Zheng X, Peng X, Zhao J, Wang X (2022) Trajectory prediction of marine moving target using deep neural networks with trajectory data. Appl Sci 12(23):11905. https://doi.org/10.3390/app122311905
80. Zhang Z, Zhao J, Wang T, Ma F, Diaconeasa MA (2023) Motion prediction of tugboats using hidden markov model. In: 2023 7th international conference on transportation information and safety (ICTIS), Xi'an, China. IEEE, New York, NY, USA, pp 621–627. https://doi.org/10.1109/ICTIS60134.2023.10243856. Accessed 17 Apr 2026
81. Zhao W, Zhang X (2023) Ship trajectory prediction with social history LSTM. In: 2023 3rd international conference on computer, control and robotics (ICCCR), Shanghai, China. IEEE, New York, NY, USA, pp 331–339. https://doi.org/10.1109/ICCCR56747.2023.10193901. Accessed 17 Apr 2026
82. Zhang J, Liu J, Li X, Han B (2023) Nonlinear and non-stationary feature processing enhanced network with transformer for ship trajectory prediction. In: 2023 International conference on machine vision, image processing and imaging technology (MVIPIT), Hangzhou, China. IEEE, New York, NY, USA, pp 181–185. https://doi.org/10.1109/MVIPIT60427.2023.00036. Accessed 17 Apr 2026
83. Li H, Jiao H, Yang Z (2023) AIS data-driven ship trajectory prediction modelling and analysis based on machine learning and deep learning methods. Transp Res Part E Logist Transp Rev 175:103152. https://doi.org/10.1016/j.tre.2023.103152
84. Cao Y, Liu J, Zhi J, Wu Z (2023) Vessel trajectory prediction based on EDA_GRU network. In: 2023 2nd international conference on machine learning, cloud computing and intelligent mining (MLCCIM), Jiuzhaigou, China. IEEE, New York, NY, USA, pp 415–419. https://doi.org/10.1109/MLCCIM60412.2023.00066. Accessed 17 Apr 2026
85. DMA (2026) AIS data—dma.dk. https://www.dma.dk/safety-at-sea/navigational-information/ais-data. Accessed 17 Apr 2026
86. Zhang Y, Han Z, Zhou X, Li B, Zhang L, Zhen E, Wang S, Zhao Z, Guo Z (2023) METO-S2S: a S2S based vessel trajectory prediction method with Multiple-semantic encoder and type-oriented decoder. Ocean Eng 277:114248. https://doi.org/10.1016/j.oceaneng.2023.114248
87. ShipFinder (2026) ShipFinder-Free satellite global ship tracking | Real-Time Marine traffic—shipfinder.com. https://www.shipfinder.com. Accessed 17 Apr 2026
88. Capobianco S, Forti N, Millefiori LM, Braca P, Willett P (2023) Recurrent encoder–decoder networks for vessel trajectory prediction with uncertainty estimation. IEEE Trans Aerosp Electron Syst 59(3):2554–2565. https://doi.org/10.1109/TAES.2022.3216823
89. Gao W, Liu J, Zhi J, Wang J (2023) Improved SocialVAE: a socially-aware ship trajectory prediction method for port operations. In: 2023 2nd international conference on machine learning, cloud computing and intelligent mining (MLCCIM), Jiuzhaigou, China. IEEE, New York, NY, USA, pp 420–424. https://doi.org/10.1109/MLCCIM60412.2023.00067. Accessed 17 Apr 2026
90. Wang X, Xiao Y (2023) A deep learning model for ship trajectory prediction using automatic identification system (AIS) data. Information 14(4):212. https://doi.org/10.3390/info14040212. (**Accessed 17.04.2026**)
91. Zhao J, Yan Z, Zhou Z, Chen X, Wu B, Wang S (2023) A ship trajectory prediction method based on GAT and LSTM. Ocean Eng 289:116159. https://doi.org/10.1016/j.oceaneng.2023.116159
92. HiFleet (2026) HiFleet—hifleet.com. https://www.hifleet.com/vessels. Accessed 17 Apr 2026
93. Spadon G, Ferreira MD, Soares A, Matwin S (2023) Unfolding AIS transmission behavior for vessel movement modeling on noisy data leveraging machine learning. IEEE Access 11:18821–18837. https://doi.org/10.1109/ACCESS.2022.3197215
94. Spire (2026) Spire: global data and analytics—spire.com. https://www.spire.com. Accessed 17 Apr 2026
95. Zhang J, Liu J, Lin T, Dai W (2024) A sequence-to-sequence based muti-semantic network with attention for long-term vessel trajectory prediction. In: 2024 2nd international conference on computer, vision and intelligent technology (ICCVIT), Huaibei, China. IEEE, New York, NY, USA, pp 1–5. https://doi.org/10.1109/ICCVIT63928.2024.10872512. Accessed 17 Apr 2026
96. Xiao Y, Luo X, Wang T, Zhang Z (2024) Spatio-temporal transformer networks for inland ship trajectory prediction with practical deficient automatic identification system data. Appl Sci 14(22):10494. https://doi.org/10.3390/app142210494
97. Dong X, Raja SS, Zhang J, Wang L (2024) Ship trajectory prediction based on CNN-MTABiGRU model. IEEE Access 12:115306–115318. https://doi.org/10.1109/ACCESS.2024.3432801
98. Bi J, Gao M, Bao K, Zhang W, Zhang X, Cheng H (2024) A CNNGRU-MHA method for ship trajectory prediction based on marine fusion data. Ocean Eng 310:118701. https://doi.org/10.1016/j.oceaneng.2024.118701
99. Zhou Y, Guo H, Lu J, Gong Z, Yu D, Ding L (2024) Using LSTM with trajectory point correlation and temporal pattern attention

for ship trajectory prediction. Electronics 13(23):4705. https://doi.org/10.3390/electronics13234705
100. Li M, Li B, Qi Z, Li J, Wu J (2024) Enhancing maritime navigational safety: ship trajectory prediction using ACoAtt–LSTM and AIS data. ISPRS Int J Geo-Inf 13(3):85. https://doi.org/10.3390/ijgi13030085
101. Shin Y, Kim N, Lee H, In SY, Hansen M, Yoon Y (2024) Deep learning framework for vessel trajectory prediction using auxiliary tasks and convolutional networks. Eng Appl Artif Intell 132:107936. https://doi.org/10.1016/j.engappai.2024.107936
102. Spadon G, Kumar J, Eden D, Berkel JI, Foster T, Soares A, Fablet R, Matwin S, Pelot R (2024) Multi-path long-term vessel trajectories forecasting with probabilistic feature fusion for problem shifting. Ocean Eng 312:119138. https://doi.org/10.1016/j.oceaneng.2024.119138
103. Ville H (Hakola). Vessel tracking (AIS), vessel metadata and dirway datasets. https://doi.org/10.21227/j3b5-es69. Accessed 17 Apr 2026
104. Han P, Zhu M, Zhang H (2024) Interaction-aware short-term marine vessel trajectory prediction with deep generative models. IEEE Trans Ind Inform 20(3):3188–3196. https://doi.org/10.1109/TII.2023.3302304
105. Wang W, Ma X, Liu B (2025) A feature-aware transformer approach for enhanced maritime trajectory prediction. In: The international conference optoelectronic information and optical engineering (OIOE2024), Wuhan, China, vol 13513. SPIE, Bellingham, WA, USA, p 135132W. https://doi.org/10.1117/12.3045838. Accessed 17 Apr 2026
106. Drapier N, Chetouani A, Chateigner A (2025) Enhancing Maritime Trajectory Forecasting via H3 Index and Causal Language Modelling (CLM). Trans Mach Learn Res 2025:1–32 https://openreview.net/forum?id=tIfS6jyO9f Accessed 17.04.2026
107. Li X, Dong D, Guo Q, Lin C, Wang Z, Ding Y (2024) A novel WTG method for predicting ship trajectories in the Fujian Inshore Area based on AIS data. Water 16(21):3036. https://doi.org/10.3390/w16213036
108. Nguyen D, Fablet R (2024) A transformer network with sparse augmented data representation and cross entropy loss for AIS-based vessel trajectory prediction. IEEE Access 12:21596–21609. https://doi.org/10.1109/ACCESS.2024.3349957
109. Takahashi K, Zama K, Hiroi NF (2024) Ship trajectory prediction using AIS data with TransFormer-based AI. In: 2024 IEEE conference on artificial intelligence (CAI), Singapore, Singapore. IEEE, New York, NY, USA, pp 1302–1305. https://doi.org/10.1109/CAI59869.2024.00230. Accessed 17 Apr 2026
110. FleetMon (2026) Live AIS vessel tracker with ship and port database—fleetmon.com. https://www.fleetmon.com. Accessed 17 Apr 2026
111. Liu H, Liu Y, Zong Z (2022) Research on ship abnormal behavior detection method based on graph neural network. In: 2022 IEEE international conference on mechatronics and automation (ICMA), Guilin, Guangxi, China. IEEE, New York, NY, USA,, pp 834–838. https://doi.org/10.1109/icma54519.2022.9856198. Accessed 17 Apr 2026
112. Dabrowski JJ, de Villiers JP (2015) Maritime piracy situation modelling with dynamic Bayesian networks. Inf Fusion 23:116–130. https://doi.org/10.1016/j.inffus.2014.07.001
113. Nominatim (2026) Nominatim Demo. https://nominatim.openstreetmap.org. Accessed 17 Apr 2026
114. rp5 (2025) Definitions—rp5.ru. https://rp5.ru. Accessed 17 Apr 2026
115. EU Copernicus Marine Service Information (CMEMS) Marine Data Store (MDS) (2024) Global ocean waves reanalysis WAVERYS. https://doi.org/10.48670/MOI-00022. Accessed 17 Apr 2026

Publisher's Note Springer Nature remains neutral with regard to jurisdictional claims in published maps and institutional affiliations.

Springer Nature or its licensor (e.g. a society or other partner) holds exclusive rights to this article under a publishing agreement with the author(s) or other rightsholder(s); author self-archiving of the accepted manuscript version of this article is solely governed by the terms of such publishing agreement and applicable law.